Heat Transfer and Fluid Flow Calculations of Industrial Shell Boilers and Evaluation of Operation Conditions – Draft

Saif-Aldain Aqel

2025

Contents

Abstract

This thesis develops a coupled combustion–heat transfer–hydraulics model for a three pass fire tube industrial shell boiler and evaluates its performance under realistic operating conditions. Implemented in Python, the modelling framework integrates (i) detailed fuel-air combustion, (ii) six sequential gas side heat exchange stages representing furnace radiation, convective tube banks, reversal chambers, and economizer, and (iii) a water/steam circuit governed by saturated boiling in the pressure parts and single phase heating in the economizer. The gas–water energy balance is solved using a one dimensional marching algorithm, which updates local heat transfer coefficients, wall temperatures, and segmental duties based on a full resistance network combining convection, radiation, fouling, and conduction.

Combustion calculations provide the adiabatic flame temperature, the fully burnt flue gas composition, and the total heat release from the lower heating value of the supplied natural gas fuel. Hydraulic losses are resolved concurrently using friction factor and minor loss correlations applied to each stage, yielding a complete gas side pressure drop profile. Boiler level performance metrics, including useful heat transfer, direct and indirect efficiencies, stack temperature, and the decomposition of radiative and convective duties, obtained after convergence of a fixed point iteration that links assumed efficiency to the resulting steam mass flow.

Sensitivity studies quantify the influence of excess air ratio, drum pressure, and firing rate on thermal performance, heat transfer distribution, pressure drop, and steam capacity. The results demonstrate that efficiency exhibits a shallow optimum near the design excess air setting; that pressure chiefly affects steam quantity rather than boiler efficiency; and that firing rate scales heat duties approximately linearly within the practical load range. The modelling framework provides a physics based tool suitable for analyzing industrial shell boiler behavior, supporting performance evaluation, operational optimization, and design exploration.

Chapter 1

Introduction

Industrial shell boilers remain one of the most widely deployed technologies for producing saturated steam and hot water in small to medium industrial plants. Their popularity arises from their compact construction, robust heat transfer surfaces, straightforward operation, and comparatively low installation and maintenance requirements. Typical applications span food and beverage processing, chemicals and pharmaceuticals, textiles, healthcare, and general manufacturing sectors where steady, reliable steam generation is essential for heating, processing, and auxiliary services.

Despite their apparent simplicity, the thermal behaviour of shell boilers is governed by tightly coupled processes: multi stage radiative and convective heat transfer, natural circulation boiling inside the pressure parts, complex flue gas property variations, and geometry dependent hydraulic losses. Modern operation demands higher efficiency, reduced emissions, increased reliability, and improved control.

This thesis develops a physics based model for a three pass fire tube shell boiler that integrates combustion calculations, detailed flue gas thermophysical properties, multi stage heat transfer modelling, and hydraulic loss estimation. The model is implemented as a one dimensional marching solver applied to six sequential heat exchange stages:

$$\mathrm{HX}_1 \rightarrow \mathrm{HX}_2 \rightarrow \mathrm{HX}_3 \rightarrow \mathrm{HX}_4 \rightarrow \mathrm{HX}_5 \rightarrow \mathrm{HX}_6,$$

representing the furnace, reversal chambers, convective tube banks, and the economiser, see figure 1.1. On the water side, the boiler drum provides a saturated interface for nucleate boiling in the pressure parts, while the economiser section is treated as a single phase internal flow. Gas side properties are supplied by Cantera, enabling temperature dependent transport, specific heat, thermal conductivity, and radiative behaviour to be modelled.

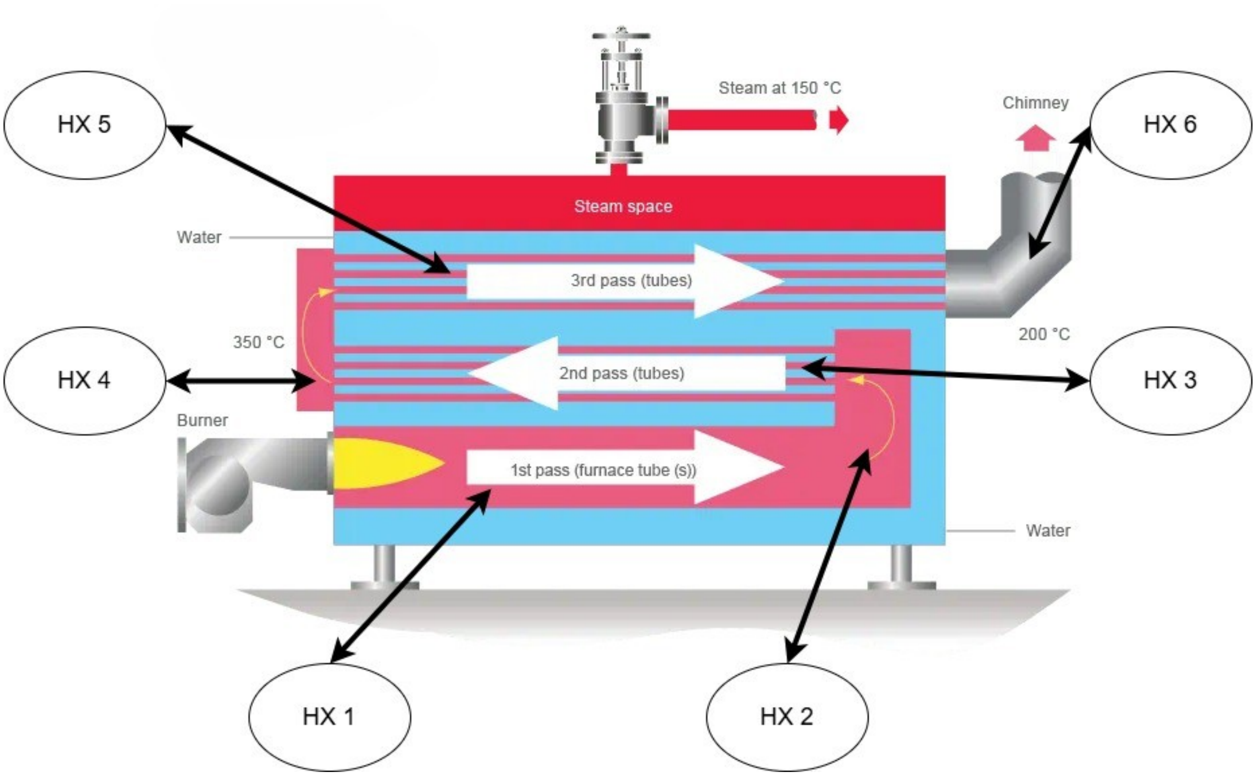

Figure 1.1: Shell boiler labeled stages.

The overall objectives of the study are:

1. To construct a unified combustion-boiler model capable of predicting flue gas temperature, composition, adiabatic flame temperature, and total heat input based on fuel composition and excess air settings.
2. To resolve heat transfer processes along the boiler using stage specific geometries, convection correlations, and a spectral based gas radiation model.
3. To quantify hydraulic losses across each pass using friction factor relations and minor loss coefficients, yielding the total boiler gas side pressure drop.
4. To compute boiler level performance, including useful heat transfer, direct and indirect efficiencies, stack temperature, and stage wise duties.
5. To evaluate sensitivity of boiler performance to key operating parameters, excess air ratio, drum pressure, and fuel mass flow rate.

The numerical framework is structured such that the water/steam mass flow is determined iteratively from the global energy balance. For each operating condition, a fixed point loop between assumed efficiency and resulting steam flow is solved until convergence, ensuring consistency between combustion input, heat transfer output, and steam generation.

The remainder of this thesis is organised as follows. Chapter 2 identifies typical industrial applications of shell boilers and introduces key design features. Chapter 3 describes the boiler geometry and outlines the six heat transfer stages. Chapter 4 develops the combustion and flue gas model, including stoichiometry and adiabatic flame temperature prediction. Chapter 5 covers the heat transfer framework, combining convection and radiation on the gas side with pool boiling and single phase correlations on the water side. Chapter 6 presents the hydraulic model. Chapter 7 reports the resulting boiler performance, while Chapter 8 examines the sensitivity of the system to variations in λ, pressure, and firing rate. Chapter 9 concludes with a summary of findings.

Chapter 2

Industrial Application of Shell Boilers

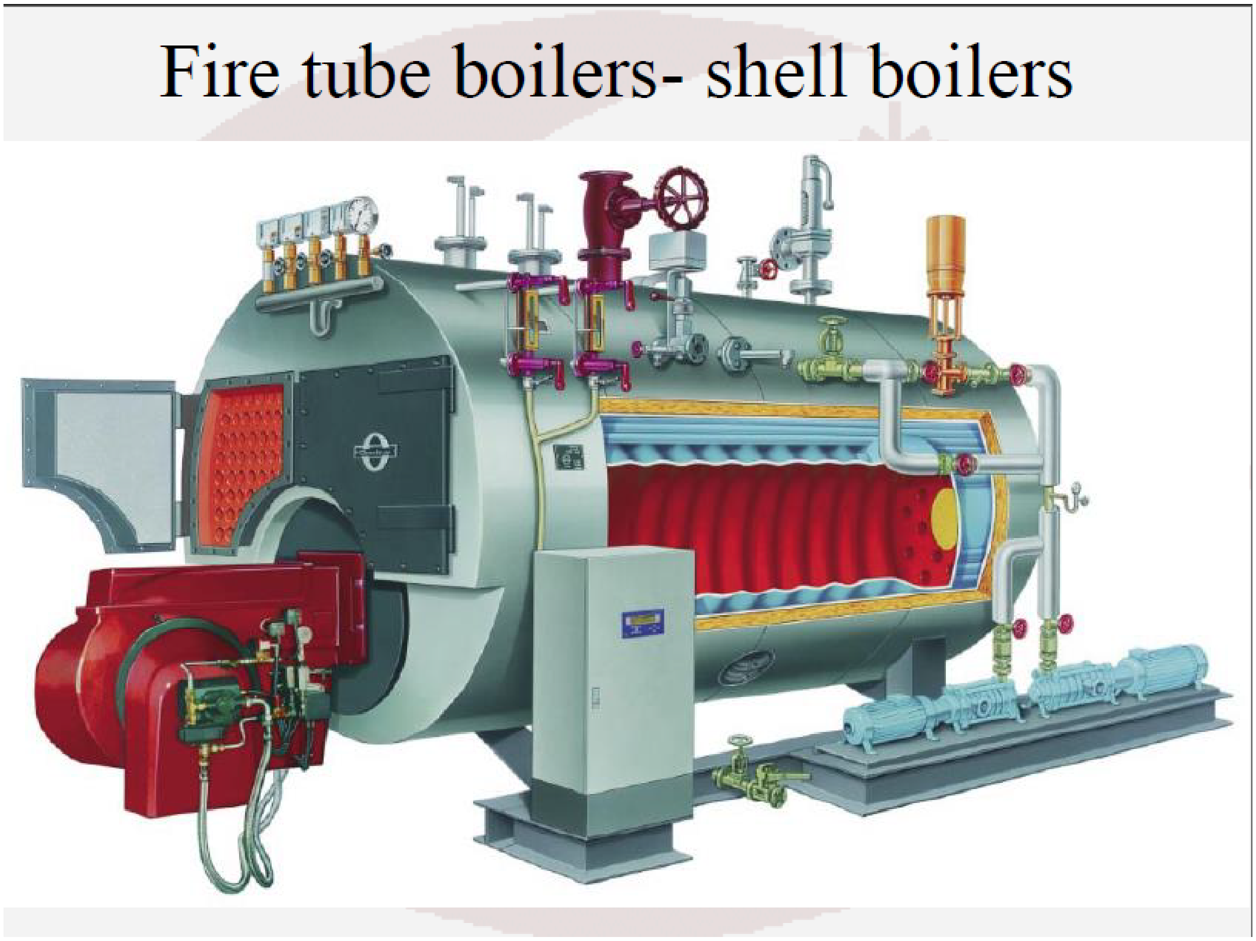

Fire tube boilers- shell boilers

Figure 2.1: Example of a packaged three-pass fire-tube shell boiler in industrial service.

2.1 Typical Industries

Shell (fire-tube) boilers are widely used in small to medium steam and hot water duties where compactness, robustness, and simple operation are prioritized over very high pressure or very large throughput. Typical sectors include:

- Food and beverage
  - Breweries, dairies, sugar refineries
  - Canneries, bakeries, confectionery plants
  - CIP (clean-in-place) systems and sterilization
- Chemical and pharmaceutical
  - Fine chemicals, specialty chemicals
  - Active pharmaceutical ingredient (API) and formulation plants
  - Steam for reactors, jacket heating, and clean steam generators
- Textiles and paper
  - Dyeing, washing, drying, and calendaring operations
  - Small paper mills and converting facilities
- Healthcare and institutional
  - Hospitals, clinics, and laboratories (space heating, humidification, sterilizers, autoclaves)
  - Universities, office complexes, district heating sub-plants
- Light manufacturing and general industry
  - Metal finishing, surface treatment, and cleaning
  - Rubber and plastics processing
  - Laundry services and commercial dry-cleaning

2.2 Standard Steam Duties

Shell boilers are normally applied in low to medium pressure ranges and moderate steam capacities:

- Typical operating pressure range:
  - Saturated steam: 6–25 bar, occasionally up to 30 bar
  - Hot-water service: 10–16 bar
- Steam-generation rates (order of magnitude):
  - Small units: 0.5–5 t/h
  - Medium units: 5–20 t/h
  - Large shell boilers (upper practical range): 20–40 t/h, beyond which water-tube designs are usually preferred

2.3 Advantages and Limitations

Advantages

- Compact and integrated construction
  - Furnace, passes, and steam/water space are combined in a single pressure body.
  - Relatively small footprint and simple installation.
- Operational simplicity
  - Straightforward start-up and shutdown procedures.
  - Typically tolerant of moderate load swings and cycling (within design limits).
  - Often delivered as packaged units with burner, controls, and safety devices pre-engineered.
- Low-to-moderate capital cost
  - Attractive for small and medium plants, boiler houses, and decentralized steam supply.
- Good part-load performance
  - Large water content provides thermal buffer, reducing short-cycling of the burner.
  - Reasonable efficiency across a wide load range, especially with economizers.
- Maintenance and inspection
  - Accessible gas passes and tube bundles (depending on design) for cleaning and inspection.
  - Long-established technology with wide service and parts availability.

Limitations

- Pressure and capacity limits
  - Practical upper bounds on shell diameter and plate thickness limit maximum pressure and steam rate.
  - For very high pressure (e.g., >40–60 bar) or very large capacities, water-tube boilers are more suitable.
- Response time
  - Large water inventory slows thermal response to rapid, large load changes compared with water-tube boilers.
- Efficiency ceiling
  - Radiative and convective heat-transfer surfaces are constrained by geometry.

  - Very high efficiencies often require additional heat-recovery equipment (economizers, condensing stages, air preheaters).

- Transport and installation constraints
  - Shell diameter and weight can be limited by route and lifting capacity.
  - Retrofitting within existing boiler houses may be constrained by overall envelope.

2.4 Multi-Pass Layout

Industrial shell boilers typically adopt multi-pass fire-tube configurations to enhance convective heat transfer and maintain acceptable gas-side velocities:

- Two-pass layout
  - First pass: large diameter furnace tube running from burner front to rear tubeplate.
  - Second pass: return of flue gas through banks of small-diameter fire-tubes back to the front tubeplate and flue outlet.
  - Simpler construction but lower total heat-transfer surface compared with three-pass designs.
- Three-pass layout (most common for industrial shell boilers)
  - Pass 1: large diameter furnace tube running from burner front to rear tubeplate.
  - Pass 2: First bank of smoke-tubes (typically reversing at the rear turnaround chamber).
  - Pass 3: Second bank of smoke-tubes.
  - Provides higher overall heat-transfer surface, more uniform gas cooling, and lower exit-gas temperatures.
- Extended heat-recovery sections
  - Economizer: additional convective heat exchanger in the flue-gas path downstream of the boiler to preheat feedwater.
  - Air preheater / condensing sections: for high-efficiency systems using suitable fuels and materials.
- Flow arrangement
  - Gas-side: burner → furnace (Pass 1) → turnaround chamber → tube bank(s) (Passes 2 and 3) → stack.
  - Water/steam side: natural circulation between heated tube surfaces and the upper steam space within the drum/shell; feedwater introduced at cooler regions (often via economizer), steam drawn from the top of the shell.

This multi-pass concept underpins the subsequent detailed modelling of each convective and radiative heat-transfer stage HX_1–HX_6 in the simulation.

Chapter 3

Configuration

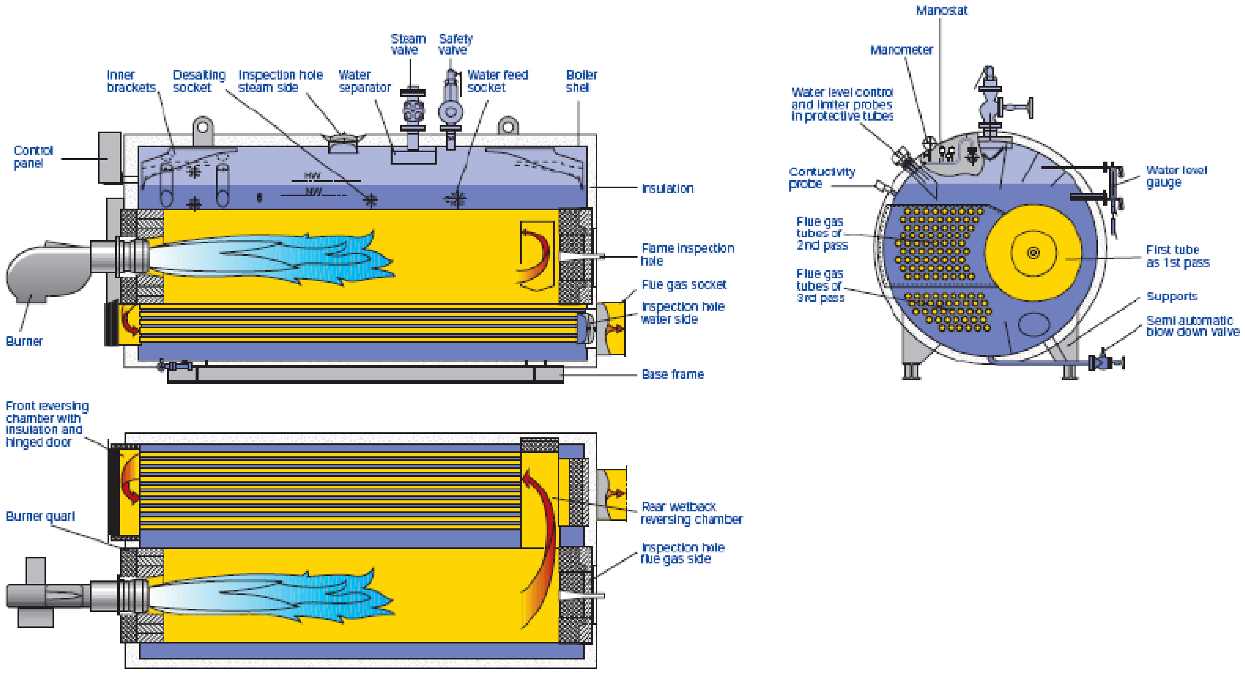
Steam valve
Safety valve
Inner brackets
Desalting socket
Inspection hole steam side
Water separator
Water feed socket
Boiler shell
Control panel
HW
NW
Insulation
Flame inspection hole
Flue gas socket
Inspection hole water side
Burner
Base frame
Front reversing chamber with insulation and hinged door
Burner quarl
Rear wetback reversing chamber
Inspection hole flue gas side
Manostat
Manometer
Water level control and limiter probes in protective tubes
Contuctivity probe
Flue gas tubes of 2nd pass
Flue gas tubes of 3rd pass
Water level gauge
First tube as 1st pass
Supports
Semi automatic blow down valve

Figure 3.1: Example of shell boiler setup components

The simulated unit is a three pass fire tube shell boiler with six distinct gas side heat transfer stages and a single common steam drum on the water/steam side. Hot flue gas from the burner traverses a radiative furnace, two reversal chambers, two convective tube banks, and a final economizer before leaving to the stack.

3.1 Layout

The gas path is represented as:

$$\text{Burner} \rightarrow HX_1 \rightarrow HX_2 \rightarrow HX_3 \rightarrow HX_4 \rightarrow HX_5 \rightarrow HX_6 \rightarrow \text{stack}$$

with the following interpretation:

- HX_1 – Furnace (first pass)
  Large, single furnace tube where combustion products enter directly from the burner and transfer heat mainly by radiation and high-temperature convection to the surrounding water/steam.
- HX_2 – First reversal chamber
  Short cylindrical wet back chamber that turns the flow from the furnace outlet into the first convective tube bank (gas direction change = 180°).
- HX_3 – First convective tube bank (second pass) Bank of small diameter fire tubes arranged in a staggered pattern inside the shell, to boost convection; flue gas flows inside of the tubes, water/steam outside.
- HX_4 – Second reversal chamber Second turning chamber redirecting gas from the first to the second tube bank.
- HX_5 – Second convective tube bank (third pass) Second fire-tube bundle, representing the last in-boiler convective pass.
- HX_6 – Economizer Separate, downstream tube bank used to preheat feedwater in single-phase operation before entering the drum/boiler circuit, recovering heat, and boosting efficiency of the boiler.

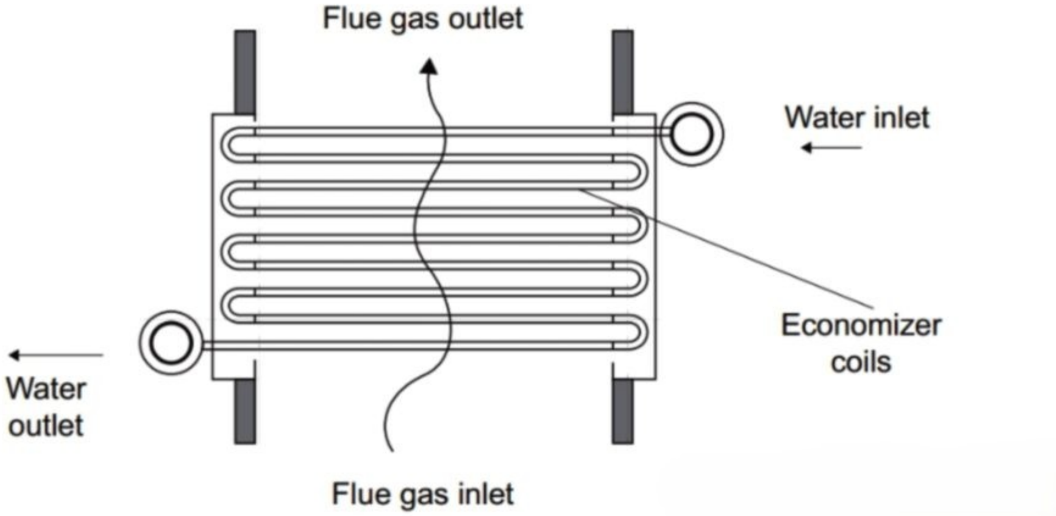

Figure 3.2: Cross-section of the economizer tube bundle HX_6, showing gas-side crossflow and water-side internal flow.

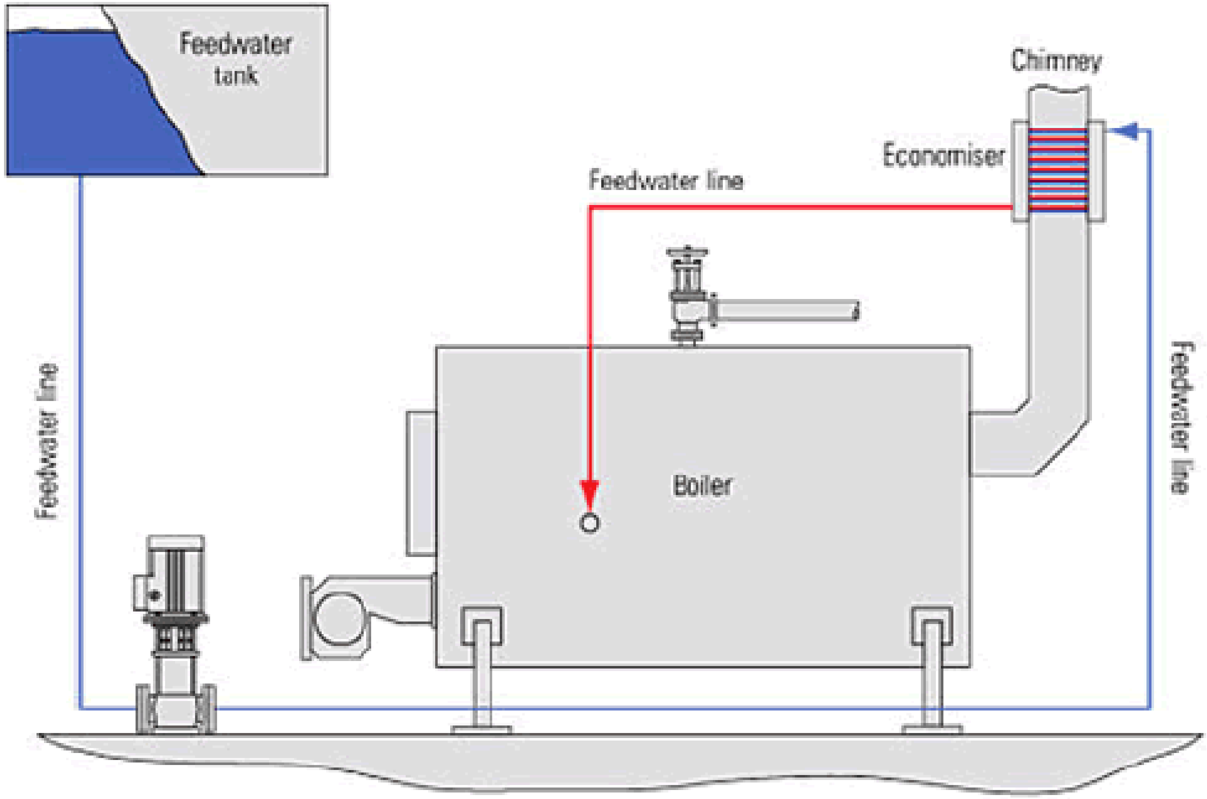

Figure 1: Economizer in Fire Tube Steam Boiler.

Figure 3.3: Three-pass shell boiler with rear-mounted economizer for feedwater preheating.

3.2 Geometry and surface specification

Drum configuration

The boiler has a single horizontal steam drum. Its inner diameter is

$$D_{i,\text{drum}} = 4.5\,\text{m}$$

and its length

$$L_{\text{drum}} = 5.0\,\text{m}$$

.

The drum is not modelled with internal separators or circulation hardware. It simply supplies the saturated water/steam state at boiler pressure, while all circulation effects are represented by the single 1-D water/steam stream used in the heat-transfer stages.

Flue gas passes

All six pressure part stages of the simulated boiler are represented with a consolidated geometric and surface specification.

Table 3.1: Flue gas stages key parameters

Element	Kind	Di [m]	L [m]	N_tubes [-]	Wall t [mm]	Roughness [µm]	Pool boiling [-]
HX_1	single_tube	1.40	5.276	1	2.9	0.5	true
HX_2	reversal_ch.	1.60	0.80	1	2.9	0.5	true
HX_3	tube_bank	0.076	4.975	118	2.9	0.5	true
HX_4	reversal_ch.	1.60	0.80	1	2.9	0.5	true
HX_5	tube_bank	0.076	5.620	100	2.9	0.5	true
HX_6	economizer	0.076	7.50	160	2.5	0.5	false

The input file `stages.yaml`, provided in Annex A, contain the complete detailed specifications and is parsed at runtime by the configuration loader (`new_loader.py`). This separates numerical solution algorithms from geometry and surface data, and allows different boiler variants to be simulated by simply modifying the YAML files.

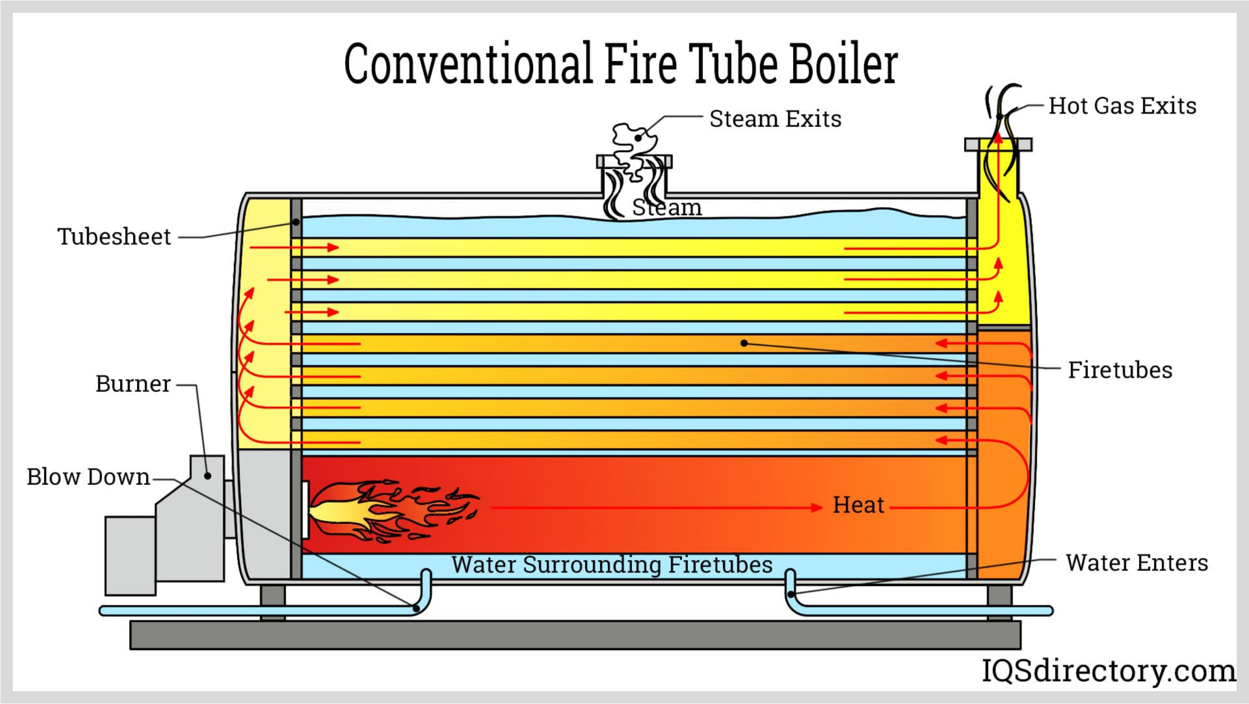

Figure 3.4: Detailed cross-section of the simulated boiler, showing drum, furnace, tube banks and reversal chambers.

All pressure-part stages (HX_1–HX_5) share the same steel wall thermal conductivity of

$\text{k}_{\text{wall}} = 16$ W/m/K. The economizer (HX_6) is modelled with a higher wall conductivity $\text{k}_{\text{wall}} = 30$ W/m/K and a clean surface (zero fouling thickness) to represent a best-case heat-recovery configuration.

The YAML configuration supplies wall, surface, and hydraulic properties not captured in the tabulated geometry. Each pressure-part exchanger defines wall thickness, wall conductivity, surface roughness, emissivity, and optional fouling layers with specified thickness and conductivity. Most stages use a uniform carbon-steel wall with smooth surfaces and thin fouling layers, while the economizer uses a thinner, higher-conductivity wall and no fouling to reflect a cleaned section.

The steam drum defines diameter, length, and internal surface properties with its own roughness and fouling settings.

Reversal chambers specify curvature radius and nozzle minor-loss coefficients used in pressure-drop calculations.

Tube-bank stages define full shell-side layout: shell diameter, tube count and pitch, tube-row arrangement (staggered or inline), baffle spacing and cut, and bundle clearances. Evaporator banks use tighter pitch and spacing to enhance shell-side transfer, whereas the economizer uses a more open inline layout with a larger tube count and longer tubes.

These YAML entries are translated by the loader into the geometric and hydraulic quantities required for cross-flow areas, Reynolds numbers, and shell-side heat-transfer evaluation.

3.3 Assumptions and limitations

1. Combustion and flue gas

   - Ideal complete combustion, with fixed excess air,
   - Adiabatic flame temperature from equilibrium chemistry, using NASA polynomials.
   - Ideal gas mixture $p = \rho RT$, with transport properties $\mu(T)\ k(T)\ c_p(T)$ from polynomial data.
   - Steady state boiler operation, with fixed fuel air and feedwater.
   - Boiler efficiency computed on HHV or LHV basis, using standard energy balance equations.

2. Heat transfer

   - One dimensional steady heat transfer per stage.
   - Uniform wall conductivity and thickness, radial conduction only.
   - Gas side HTC from standard correlations properties **vary** with temperature pressure and composition.
   - Gas radiation via band averaged grey model for CO_2 and H_2O, no spectral resolution, and no soot formation.
   - Water side HTC uses IAPWS-IF97 properties, homogenized two phase model.
   - Drum at fixed pressure, and perfect steam water separation (no carryover).

3. Hydraulic and thermal performance

   - 1D, steady, single phase flow.
   - Constant mass flow along each stage.
   - Compressibility effects appear only through property variations $\rho(T, P)$ and $\mu(T, P)$ in Re and $\rho V^2/2$.
   - Stage level minor loss coefficients are lumped, and uniformly distributed along the stage.
   - Gas side ΔP in economizer stage is neglected.

Chapter 4

Combustion Model

The combustion module forms the first stage of the design workflow. It reads all run-specific configurations and parameters from YAML files and simulates the combustion process for the specified fuel and air streams at the given excess air ratio. Its outputs are the adiabatic flame temperature, used as the inlet temperature for the flue gas entering the first pass, and the fully combusted flue gas composition. Together, these results define the flue-gas stream supplied to the heat-transfer model.

4.1 Fuel Stream

The boiler is fired with a natural-gas–type fuel defined in the simulation input (`config/fuel.yaml`).
The fuel is supplied at $300K$ and $1.013 \times 10^5 Pa$ with a mass flow rate of $0.1kg/s$.
Its composition is specified on a mass-fraction basis and converted internally to mole fractions for all stoichiometric and thermodynamic calculations.

Table 4-1 summarizes the fuel composition in both mass and mole fraction form.

		Mass fraction	Mole fraction	
Component	Formula	w_i [-]	x_i [-]	Comment
Methane	CH_4	0.80	0.8895	Main combustible, dominant contributor to LHV
Ethane	C_2H_6	0.10	0.0593	Heavier hydrocarbon, increases LHV and required O_2
Propane	C_3H_8	0.04	0.0162	Heavier hydrocarbon, raises flame temperature
n-Butane	C_4H_{10}	0.01	0.00307	Minor heavy hydrocarbon fraction

		Mass fraction	Mole fraction	
Component	Formula	w_i [-]	x_i [-]	Comment
Hydrogen sulfide	H_2S	0.01	0.00523	Sulfur-bearing contaminant → SO_2 in flue gas
Nitrogen	N_2	0.02	0.0127	Inert ballast in the fuel stream
Carbon dioxide	CO_2	0.01	0.00405	Inert (already fully oxidized)
Water vapour	H_2O	0.01	0.00990	Moisture carried with the fuel

The mass fractions sum to 1.0 by definition. The mole fractions x_i are obtained from

$$x_i = \frac{\frac{w_i}{M_i}}{\sum_j \frac{w_j}{M_j}}$$

which is provided by the function `to_mol` in `combustion/mass_mole.py`, where M_i is the molar mass of species i from `molar_masses` in `common/constants.py`.

4.2 Air Stream

4.3 Model flow

The purpose of the combustion model is to determine combustion conditions inside the furnace (1st pass), resulting in a fully burnt flue gas stream entering the heat transfer model at adiabatic temperature.

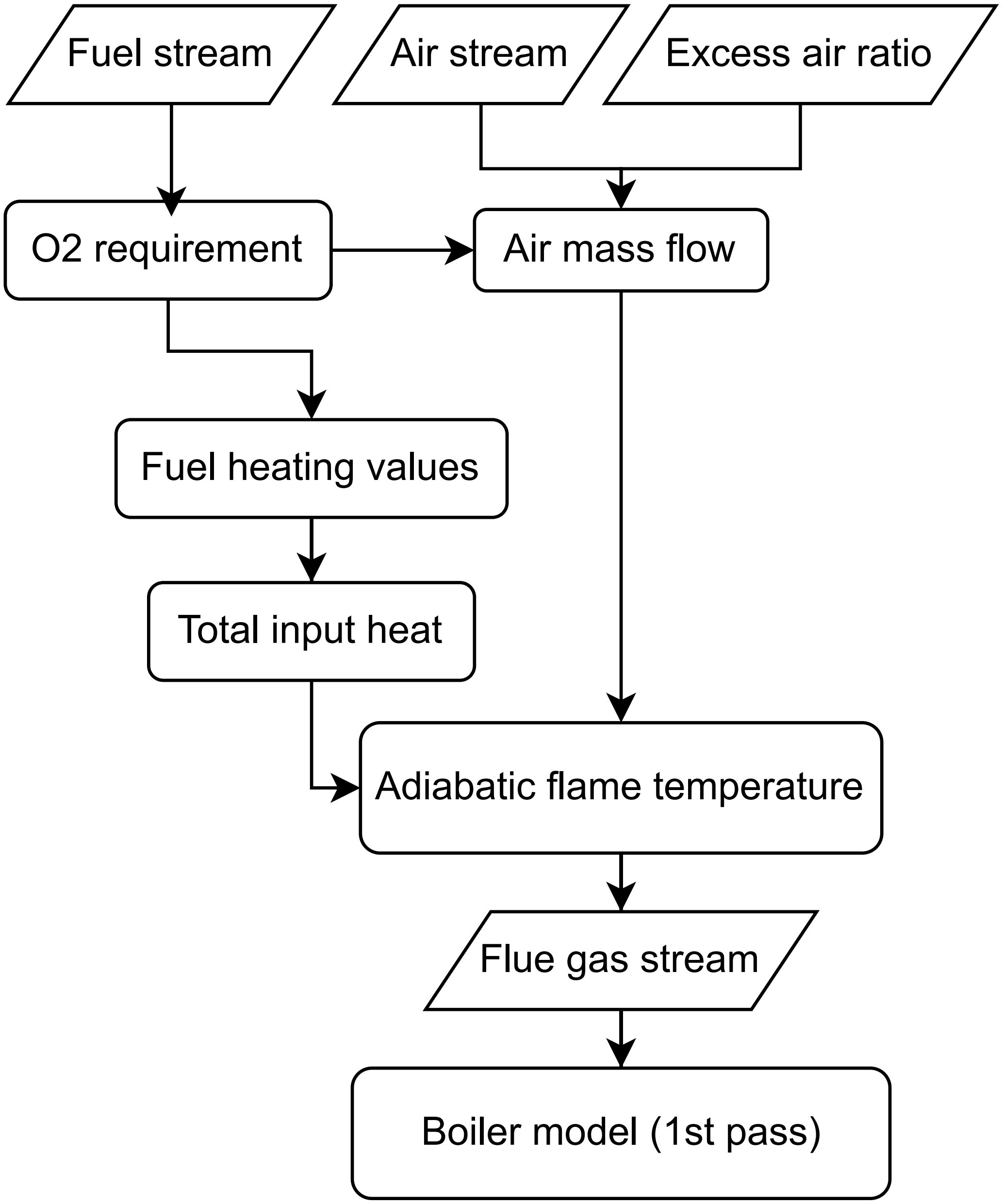

Figure 4.1: Combustion flow

4.4 Stoichiometric O_2 requirement

Evaluated the stoichiometric oxygen requirement via `stoich_O2_required_per_mol_fuel` in `combustion/flue.py`. The algorithm is:

1. Use per mole of species stoichiometric O_2 factors $\nu_{O_{2,i}}$ from `O2_per_mol` in `common/constants.py`:

Species	Global reaction (complete combustion)	$\nu_{O_2,i}$ [mol O_2 / mol species]
CH_4	CH_4 + 2 O_2 → CO_2 + 2 H_2O	2.0
C_2H_6	C_2H_6 + 3.5 O_2 → 2 CO_2 + 3 H_2O	3.5
C_3H_8	C_3H_8 + 5 O_2 → 3 CO_2 + 4 H_2O	5.0
C_4H_{10}	C_4H_{10} + 6.5 O_2 → 4 CO_2 + 5 H_2O	6.5
H_2S	H_2S + 1 O_2 → SO_2 + H_2O	1.0
N_2, CO_2, H_2O	Inert/fully oxidized → no additional O_2	0.0

2. Compute the stoichiometric O_2 requirement per mole of fuel mixture as

$$\nu_{O_2,\text{stoich}} = \sum_i x_i \, \nu_{O_2,i}$$

Using the mole fractions from Section 4.1 for the present fuel:

- $x_{CH_4} = 0.8895$
- $x_{C_2H_6} = 0.0593$
- $x_{C_3H_8} = 0.0162$
- $x_{C_4H_{10}} = 0.00307$
- $x_{H_2S} = 0.00523$
- remaining species: x_{N_2}, x_{CO_2}, x_{H_2O} are inert in the stoichiometric balance.

Hence

$$\nu_{O_2,\text{stoich}} = 2.09 \;\; \text{mol } O_2 \text{ per mol fuel mixture}$$

This is exactly what `stoich_O2_required_per_mol_fuel` returns:

```python
def stoich_O2_required_per_mol_fuel(fuel: GasStream) -> Q_:
    fuel_x = to_mole(fuel.comp)
    total = sum(fuel_x[k] * O2_per_mol.get(k, 0.0) for k in fuel_x)
    return Q_(total, ”dimensionless”)
```

3. For later hydraulic and performance interpretation, it is also useful to express this on a mass basis.

   For 1 kg of fuel, the total fuel moles are

   $$\text{n}_{\text{fuel,total}} = \sum_i \frac{w_i}{M_i} = 56.1 \text{ mol fuel/kg}$$

   Thus the stoichiometric O_2 requirement per unit fuel mass is

   $$n^{(m)}_{\text{O}_2\text{,stoich}} = \nu_{\text{O}_2\text{,stoich}}\, n_{\text{fuel,total}} = 1.17 \times 10^2 \text{ mol O}_2\text{/kg fuel}$$

   Converting to mass of O_2 per kg of fuel:

   $$\dot{m}_{\text{O}_2\text{,stoich}} = n^{(m)}_{\text{O}_2\text{,stoich}} M_{\text{O}_2} = 3.75 \text{ kg O}_2\text{/kg fuel}$$

So, for this fuel:

- Stoichiometric oxygen requirement:
  $\boxed{\nu_{\text{O}_2\text{,stoich}} = 2.09 \text{ mol O}_2 \text{ per mol fuel mixture}}$
- Equivalent mass requirement:
  $\boxed{\dot{m}_{\text{O}_2\text{,stoich}} = 3.75 \text{ kg O}_2 \text{ per kg fuel}}$

4.5 Air–fuel ratio and excess air λ

The simulation specifies an excess air ratio

$$\lambda = 1.1$$

in `config/operation.yaml`. This value enters the calculation through `air_flow_rates(air, fuel, excess)` in `combustion/flue.py`.

4.5.1 Actual O_2 supplied

Using:

$$\dot{n}_{\text{O}_2\text{,actual}} = \lambda\, \dot{n}_{\text{O}_2\text{,stoich}}$$

Thus:

$$\dot{n}_{\text{O}_2\text{,actual}} = 1.1\, \nu_{\text{O}_2\text{,stoich}}\, \dot{n}_{\text{fuel}}$$

The molar fuel flow is determined from the mass-flow rate:

- Fuel mass flow:

$$\dot{m}_f = 0.5 \text{ kg/s}$$

- Total moles per unit mass of fuel mixture (from the mixture molar mass calculation):

$$n_{\text{fuel,total}} = 56.1 \text{ mol/kg}$$

- Therefore the total molar fuel flow:

$$\dot{n}_f = 56.1 \times 0.5 = 28.05 \text{ mol/s}$$

Hence the stoichiometric and actual O_2 flows are:

$$\dot{n}_{O_2,\text{stoich}} = 2.09 \times 28.05 = 58.7 \text{ mol/s}$$

$$\dot{n}_{O_2,\text{actual}} = 1.1 \times 58.7 = 64.6 \text{ mol/s}$$

4.5.2 Air required

Air O_2 mole fraction (from `air.yaml`):

$$x_{O_2,\text{air}} = 0.2095$$

Thus:

$$\dot{n}_{\text{air}} = \frac{\dot{n}_{O_2,\text{actual}}}{x_{O_2,\text{air}}} = \frac{64.6}{0.2095} = 308 \text{ mol/s}$$

The air molar mass (mixture weighted) is:

$$M_{\text{air}} = 0.02897 \text{ kg/mol}$$

Therefore the mass-based air flow rate:

$$\dot{m}_{\text{air}} = \dot{n}_{\text{air}} M_{\text{air}} = 308 \times 0.02897 = 8.93 \text{ kg/s}$$

4.5.3 Air–fuel ratio

Mass-based air–fuel ratio:

$$\text{AFR} = \frac{\dot{m}_{\text{air}}}{\dot{m}_f} = \frac{8.93}{0.5} = 17.9$$

4.6 Lower heating value (LHV) and heat release

The fuel lower and higher heating values, and the corresponding firing rate, are evaluated in `combustion/heat.py` by the function `compute_LHV_HHV(fuel)` and then used by `total_input_heat(fuel, air)`.

4.6.1 Method

4.6.1.1 Latent heat of water

Obtain the latent heat of vaporization of water at the reference pressure $P_{\text{ref}} = 101{,}325$ Pa from the IAPWS-97 correlation:

```
latent_H2O = WaterProps.h_g(P_ref) - WaterProps.h_f(P_ref)
```

where:

- h_g is the saturated vapour enthalpy,
- h_f is the saturated liquid enthalpy.

4.6.1.2 Reference formation enthalpies

Standard formation enthalpies $\Delta h_{\text{f}}^{\circ}$ (at 298.15 K, 1 bar) are taken from `common/constants.py` in kJ/mol:

Table 4.1: Standard enthalpy of formation of selected species (Johnson et al. 2024)

Species	$\Delta h_{\text{f}}^{\circ}$ (kJ mol^{-1})
CH_4	–74.8
C_2H_6	–84.7
C_3H_8	–103.8
C_4H_{10}	–126.1
SO_2	–296.8
CO_2	–393.5
$H_2O(l)$	–285.5

4.6.1.3 Products for HHV and LHV

For each fuel species, complete combustion is considered:

- $CH_4 + 2\,O_2 \rightarrow CO_2 + 2\,H_2O$
- $C_2H_6 + 3.5\,O_2 \rightarrow 2\,CO_2 + 3\,H_2O$

Builds product formation enthalpies for:

- HHV assumption: water as liquid (condensed)
- LHV assumption: water as vapour (no condensation heat recovered)

```
H2O_liq = _dHf[”H2O”]                       # kJ/mol
H2O_vap = _dHf[”H2O”] + latent_H2O * M_H2O  # (kJ/kg)*(kg/mol) = kJ/mol
```

Then, looping over the *molar* fuel composition `mol_comp = to_mole(fuel.comp)`:

```
react = 0
HHV_p = 0
LHV_p = 0

for comp, x in mol_comp.items():
    dh = _dHf.get(comp, 0)
    react += x * dh

    C, H = parse_CH(comp)
    if C is not None:
        HHV_p += x * (C * _dHf[”CO2”] + (H/2) * H2O_liq)
        LHV_p += x * (C * _dHf[”CO2”] + (H/2) * H2O_vap)
    elif comp == ”H2S”:
        HHV_p += x * (_dHf[”SO2”] + H2O_liq)
        LHV_p += x * (_dHf[”SO2”] + H2O_vap)
    else:
        HHV_p += x * dh
        LHV_p += x * dh
```

Here:

- `react` represents the mixture-averaged formation enthalpy of the fuel (kJ/mol),
- `HHV_p`, `LHV_p` represent the mixture-averaged formation enthalpy of the ideal products for HHV and LHV definitions.

4.6.1.4 Mixture HHV and LHV (molar, then mass-based)

The mixture molar higher and lower heating values are:

$$\text{HHV}_{\text{mol}} = h_{\text{react}} - h_{\text{prod,HHV}}, \quad \text{LHV}_{\text{mol}} = h_{\text{react}} - h_{\text{prod,LHV}}$$

```
HHV_mol = react - HHV_p      # kJ/mol
LHV_mol = react - LHV_p      # kJ/mol
```

These are converted to mass-based heating values using the mixture molar mass M_{mix} from `mix_molar_mass(mol_comp)`:

```
HHV_kg  = HHV_mol / M_mix   # kJ/kg
LHV_kg  = LHV_mol / M_mix   # kJ/kg
```

The function returns these, together with the corresponding firing powers:

```
P_HHV = (HHV_kg * fuel.mass_flow).to(”kW”)
P_LHV = (LHV_kg * fuel.mass_flow).to(”kW”)
```

4.6.2 Numerical results for the present fuel

For the fuel specified above, the mixture heating values are:

- Higher heating value (HHV, mass-based):

$$\text{HHV}_{\text{mix}} = 52\,\text{MJ/kg}$$

- Lower heating value (LHV, mass-based):

$$\text{LHV}_{\text{mix}} = 47\,\text{MJ/kg}$$

For the specified fuel mass flow rate:

$$\dot{m}_f = 0.5\ \text{kg/s}$$

the resulting firing rates are:

- On an HHV basis:

$$P_{\text{HHV}} = \dot{m}_f\,\text{HHV}_{\text{mix}} = 0.5 \times 52\ \text{MJ/s} = 26\ \text{MW}$$

- On an LHV basis (used consistently in the simulation):

$$P_{\text{LHV}} = \dot{m}_f\,\text{LHV}_{\text{mix}} = 0.5 \times 47\ \text{MJ/s} = 23.6\ \text{MW}$$

These correspond directly to `P_HHV` and `P_LHV` returned by `compute_LHV_HHV`.

4.6.3 Total heat input to the boiler Q_{in}

The function `total_input_heat(fuel, air)` combines chemical and sensible contributions:

```
def total_input_heat(fuel, air):
    _, _, _, power_LHV = compute_LHV_HHV(fuel)
    fuel_sens = sensible_heat(fuel)
    air_sens  = sensible_heat(air)
    Q_in = (power_LHV + fuel_sens + air_sens).to(”kW”)
    return power_LHV, Q_in
```

where `sensible_heat(stream)` uses:

$$Q_{\text{sens}} = \dot{m}\, c_p\, (T - T_{\text{ref}})$$

Both fuel and air enter at 300 K, while the reference is 298.15 K; the resulting sensible contributions are small compared with the chemical term P_{LHV} (on the order of tens of kW versus tens of MW). Therefore, numerically:

- LHV-based chemical heat input:

$$P_{\text{LHV}} = 23.6 \text{ MW}$$

- Total heat input including sensible:

$$Q_{\text{in}} = P_{\text{LHV}} + Q_{\text{sens,fuel}} + Q_{\text{sens,air}} = 23.6 \text{ MW} \quad (\text{increase } < 0.1\%)$$

The quantity `Q_in` in the `CombustionResult` object is thus interpreted in the rest of the boiler model as the total LHV-based heat release available to be transferred to the water/steam side.

4.7 Adiabatic flame temperature

The adiabatic flame temperature T_{ad} is evaluated in the model by the function `adiabatic_flame_T(air, fuel)` in `combustion/adiabatic_flame_temperature.py`. This routine uses Cantera and an enthalpy–pressure equilibrium (`HP`) calculation to determine the final equilibrium temperature and composition of the flue gas, assuming:

- complete mixing of fuel and air,
- no heat losses to the surroundings (adiabatic),
- constant system pressure (equal to the air/fuel inlet pressure),
- chemical equilibrium among all gas species in `config/flue_cantera.yaml`.

4.7.1 Thermodynamic formulation

Let the fuel and air streams be characterized by:

- mass flows $\dot{m}_{\text{fuel}}, \dot{m}_{\text{air}}$,
- inlet temperatures $T_{\text{fuel}}, T_{\text{air}}$,

- pressure P,
- compositions (mole fractions) $X_{\text{fuel}}, X_{\text{air}}$.

The total inlet enthalpy rate of the unmixed reactants is

$$\dot{H}_{\text{react}} = \dot{m}_{\text{air}}\, h_{\text{air}}(T_{\text{air}}, P, X_{\text{air}}) + \dot{m}_{\text{fuel}}\, h_{\text{fuel}}(T_{\text{fuel}}, P, X_{\text{fuel}})$$

The total mass flow is

$$\dot{m}_{\text{tot}} = \dot{m}_{\text{air}} + \dot{m}_{\text{fuel}}$$

so the mixture-averaged specific enthalpy of the reactants is

$$h_{\text{target}} = \frac{\dot{H}_{\text{react}}}{\dot{m}_{\text{tot}}}$$

The adiabatic, constant-pressure equilibrium state is then defined by the constraints:

$$\begin{aligned} h_{\text{products}}(T_{\text{ad}}, P, \mathbf{X}_{\text{eq}}) &= h_{\text{target}} \\ P_{\text{out}} &= P \\ \mathbf{X}_{\text{eq}} &\text{ satisfies chemical equilibrium at } (T_{\text{ad}}, P) \end{aligned}$$

Cantera is used to enforce this condition via its `HP` equilibrium mode.

4.7.2 Implementation

Key steps from `adiabatic_flame_T`:

1. Convert the mass-based composition of fuel and air to mole fractions using `to_mole(...)` (from `combustion/mass_mole.py`).
2. Create three Cantera `Solution` objects using the mechanism `config/flue_cantera.yaml`:

```
gas_air   = ct.Solution("config/flue_cantera.yaml", "gas_mix")
gas_fuel  = ct.Solution("config/flue_cantera.yaml", "gas_mix")
gas_mix   = ct.Solution("config/flue_cantera.yaml", "gas_mix")
```

3. Set the inlet states of the separate streams:

```
gas_air.TPX   = T_air,  P_Pa, X_air
gas_fuel.TPX  = T_fuel, P_Pa, X_fuel
```

4. Compute reactant enthalpy rate and target specific enthalpy:

```
Hdot_react = m_air * gas_air.enthalpy_mass + m_fuel * gas_fuel.enthalpy_mass
h_target   = Hdot_react / m_tot           # J/kg of mixture
```

5. Build the overall reactant composition $\mathbf{X}_{\text{react}}$ from the molar flow rates of each component in each stream:

```
n_air  = molar_flow(air.comp,  air.mass_flow)
n_fuel = molar_flow(fuel.comp, fuel.mass_flow)

# Accumulate species molar flow rates
n_dot_sp = {...}
X_react = {k: v / n_sum for k, v in n_dot_sp.items()}
```

6. Initialize the mixture and perform HP equilibrium:

```
gas_mix.TPX = 300.0, P_Pa, X_react   # initial guess for T
gas_mix.HP  = h_target, P_Pa         # enforce (H,P)
gas_mix.equilibrate(”HP”)            # chemical equilibrium
```

7. Construct the resulting flue-gas stream:

```
Y_eq = gas_mix.Y  # equilibrium mass fractions
comp_eq = {sp: Q_(float(Y_eq[i]), ””) for i, sp in enumerate(gas_mix.species_names)
           if Y_eq[i] > 1e-15}

flue = GasStream(
    mass_flow = Q_(m_tot, ”kg/s”),
    T         = Q_(gas_mix.T, ”K”),
    P         = air.P,
    comp      = comp_eq,
)
```

The adiabatic flame temperature is then available as `flue.T` and is also stored in `CombustionResult.T_ad`.

4.7.3 Numerical result for the present case

For the given conditions:

- Fuel: natural-gas–type mixture from Section 4.1, $\dot{m}_{\text{fuel}} = 0.5$ kg/s, $T_{\text{fuel}} = 300$ K, 1.013×10^5 Pa.
- Air: dry air at 300 K and 1.013×10^5 Pa, composition from `config/air.yaml`.
- Excess air: $\lambda = 1.1$ (10 % excess air).

the HP-equilibrium calculation yields an adiabatic flame temperature on the order of:

$$T_{\text{ad}} \;=\; 2{,}050\,\text{K} \quad (= 1{,}780^{\circ}\text{C})$$

This value is consistent with typical adiabatic flame temperatures for natural gas with around 10 % excess air and confirms that the combustion zone (furnace) operates at very high gas temperatures, driving strong radiative and convective heat transfer to the shell-side water/steam.

The scalar `T_ad` is passed forward and written into the boiler summary CSV (`*_boiler_summary.csv`) for reference and later comparison with non-adiabatic stack temperatures obtained from the full boiler simulation.

4.8 Flue gas composition

In the combustion model two different flue gas streams are distinguished:

1. An equilibrium flue gas at adiabatic flame conditions (`flue_ad`), obtained from high temperature HP equilibrium in Cantera.
2. A fully burnt boiler flue gas (`flue`), obtained from pure stoichiometry with excess air and no dissociation, used throughout the heat-exchanger network.

Both are represented as `GasStream` objects and stored in the `CombustionResult`, but they serve different purposes in the boiler calculation.

4.8.1 Definitions and distinction

- **Equilibrium flue gas (`flue_ad`)**
  - Thermodynamic state: high temperature HP equilibrium at the adiabatic flame temperature.
  - Contains all equilibrium species allowed by the mechanism (major products + dissociation products + radicals).
  - Used only to:
    - determine the adiabatic flame temperature T_{ad},
    - report equilibrium composition in diagnostics/CSV.
- **Fully burnt flue gas (`flue`)**
  - Thermodynamic state: chemically frozen, fully burnt mixture at the same temperature and pressure as the equilibrium gas at burner exit.
  - Contains only “engineering” products ($C\mathrm{O}_2$, H_2O, $S\mathrm{O}_2$, O_2, N_2, Ar) with no CO, H_2, $N\mathrm{O}_x$ or radicals.
  - Used as the hot-side gas in all boiler heat-transfer and pressure-drop calculations.

Hence, equilibrium chemistry is confined to the flame-temperature calculation, while the boiler itself is solved with a simplified, fully burnt flue gas consistent with complete combustion and 10 % excess air.

4.8.2 Equilibrium flue gas at adiabatic conditions

The adiabatic flame calculation is performed in `combustion/adiabatic_flame_temperature.py` via the function `adiabatic_flame_T(air, fuel)`:

- The inlet air and fuel streams are:
  - represented as `GasStream` objects (mass flow, T, P, mass fractions),
  - converted to mole fractions (`to_mole`) and set into separate Cantera `Solution` objects (`gas_air`, `gas_fuel`) based on `config/flue_cantera.yaml`.
- A mixed-reactant state is constructed at constant pressure:
  - Total enthalpy flow of reactants:

$$\dot{H}_{\text{react}} = \dot{m}_{\text{air}}\, h_{\text{air}} + \dot{m}_{\text{fuel}}\, h_{\text{fuel}}$$

  - Target specific enthalpy:

$$h_{\text{target}} = \dot{H}_{\text{react}} / \dot{m}_{\text{tot}}$$

  - Overall reactant mole fractions are built from molar flow rates of air and fuel.
- The mixture is then set in Cantera (`gas_mix`) with:
  - composition X_{react},
  - pressure $P = P_{\text{air}}$,
  - specific enthalpy $h = h_{\text{target}}$,
  - and equilibrated under HP constraints:

```
gas_mix.TPX = 300.0, P_Pa, X_react   # T placeholder
gas_mix.HP  = h_target, P_Pa
gas_mix.equilibrate(”HP”)
```

- After equilibrium:
  - The **adiabatic flame temperature** is `gas_mix.T`.
  - The **equilibrium mass fractions** are read from `gas_mix.Y`:

```
Y_eq = gas_mix.Y
comp_eq = {
    sp: Q_(float(Y_eq[i]), ””)
    for i, sp in enumerate(gas_mix.species_names)
    if Y_eq[i] > 1e-15
}
```

- These are stored in the equilibrium flue-gas stream:

```
flue_ad = GasStream(
    mass_flow = Q_(m_tot, ”kg/s”),
    T         = Q_(gas_mix.T, ”K”),
    P         = air.P,
    comp      = comp_eq,
)
```

Typical equilibrium composition (λ = 1.1, natural gas, $T_{\text{ad}} = 2050$ K) is:

- Major species:
  - CO_2 ≈ 0.085–0.095
  - H_2O ≈ 0.075–0.085
  - O_2 ≈ 0.020–0.030 (excess air)
  - N_2 ≈ 0.78–0.80
- Dissociation / minor species:
  - CO ≈ 10^{-3}
  - H_2 ≈ 10^{-4}
  - NO ≈ 10^{-4}–10^{-5}
  - OH, O, radicals < 10^{-6}
  - SO_2 = 10^{-4} (from fuel H_2S)

This composition is physically consistent with high-temperature equilibrium at $2000K$ and slight dissociation.

The object `flue_ad` is stored in `CombustionResult` and is only used to:

- provide T_{ad} and equilibrium composition to the boiler summary CSV,
- support diagnostic post processing.

It is **not** used in the heat exchanger network.

4.8.3 Fully burnt boiler flue gas

The boiler thermal model requires a chemically simple flue-gas mixture to compute heat transfer and pressure drop. For that purpose a **fully burnt** flue gas is constructed in `combustion/flue.py` and `combustion/combustor.py`:

1. In `Combustor.run()` the air mass flow is first set from stoichiometry plus excess air:

   ```
   air.mass_flow = air_flow_rates(air, fuel, self.excess_air_ratio)
   ```

2. The fully burnt flue-gas composition is then computed from pure stoichiometry:

   ```
   mass_comp_burnt, m_dot_flue = from_fuel_and_air(fuel, air)
   ```

   - `from_fuel_and_air` assumes complete oxidation of:
     - C-containing species → CO_2,
     - H → H_2O,
     - S → SO_2,
   - including CO_2 and H_2O already present in the inlet fuel and air.

   - The allowed product set is:
     - CO_2, H_2O, SO_2, O_2, N_2, Ar.
   - Residual O_2 is determined by the imposed excess air ratio λ; there is no CO, H_2, NO_x, or radicals in this stream.

   Internally, `from_fuel_and_air` works with molar balances:

   - determines stoichiometric O_2 demand per mole of fuel (`stoich_O2_required_per_mol_fuel`),
   - combines fuel and air mole fractions to get:

   $$\dot{n}_{CO_2},\ \dot{n}_{H_2O},\ \dot{n}_{SO_2},\ \dot{n}_{O_2},\ \dot{n}_{N_2},\ \dot{n}_{Ar}$$

   - normalizes by total moles to obtain mole fractions, converts to mass fractions (`to_mass`), and returns both:
     - `mass_comp` (mass fractions),
     - `m_dot` (total mass flow of flue gas).

3. The fully burnt flue-gas stream is then created as:

   ```
   flue_boiler = GasStream(
       mass_flow = Q_(m_dot_flue, ”kg/s”),
       T         = T_ad,     # assume recombination to near Tad at burner exit
       P         = air.P,
       comp      = {sp: Q_(y, ””) for sp, y in mass_comp_burnt.items()},
   )
   ```

4. `CombustionResult` is populated with both flue streams:

   ```
   return CombustionResult(
       LHV          = power_LHV,
       Q_in         = Q_in,
       T_ad         = T_ad,
       flue         = flue_boiler,  # fully burnt flue used in boiler model
       flue_ad      = flue_ad,      # equilibrium flue at Tad (diagnostics)
       fuel_LHV_mass  = LHV_mass,
       fuel_P_LHV     = P_LHV,
   )
   ```

The **boiler solver** (`run_hx`) always receives `combustion.flue` (i.e. `flue_boiler`) as its gas inlet, and this fully burnt composition is used for:

- gas properties (`cp`, ρ, μ, k),
- heat-transfer coefficients,
- radiative heat transfer (emissivity based on CO_2/H_2O/SO_2),
- pressure-drop estimates and stack temperature.

Thus, the equilibrium flue gas provides a physically consistent high-temperature reference, while the fully burnt flue gas represents the practical working fluid in the convective–radiative sections of the boiler.

4.8.4 Output fields

The flue-gas information exposed to the rest of the model and to the post-processing is encapsulated in `CombustionResult`:

```
@dataclass(frozen=True)
class CombustionResult:
    LHV: Q_
    Q_in: Q_
    T_ad: Q_
    flue: GasStream                 # fully-burnt flue used in boiler
    flue_ad: GasStream | None = None    # equilibrium flue at T_ad (optional)
    fuel_LHV_mass: Q_ | None = None
    fuel_P_LHV: Q_ | None = None
```

The relevant report/CSV entries are:

Field	Meaning
`T_ad`	Adiabatic flame temperature from HP equilibrium
`flue_ad`	`GasStream` of equilibrium flue gas (adiabatic composition, diagnostics)
`flue`	`GasStream` of fully burnt flue gas used in all boiler HX calculations

This completes the description of how flue-gas composition is defined, distinguished, and used in the boiler model.

Chapter 5

Heat Transfer Model

5.1 Fundamental heat-balance equations

The boiler is modelled as a one-dimensional counter-current heat exchanger composed of six stages (HX_1–HX_5). Heat transfer is resolved along the gas flow direction x, while water flows in the opposite direction. Each stage is discretized into segments of length $\mathrm{d}x$; all local quantities are defined per unit length.

- Notation (per segment)
- x – axial coordinate along the gas flow [m]
- $\mathrm{d}x$ – marching step in x [m]
- $\dot{m}_g, \dot{m}_w$ – gas and water mass flow rates [kg/s]
- $T_g(x),\, T_w(x)$ – bulk gas and water temperatures [K]
- $T_{gw}(x),\, T_{ww}(x)$ – gas-side and water-side wall temperatures [K]
- $h_g(x),\, h_w(x)$ – total gas-side and water-side heat-transfer coefficients [W/m²·K]
- P_g, P_w – gas-side and water-side wetted perimeters [m]
- $q'(x)$ – linear heat flux (heat per unit length) [W/m]
- $UA'(x)$ – overall conductance per unit length [W/K/m]

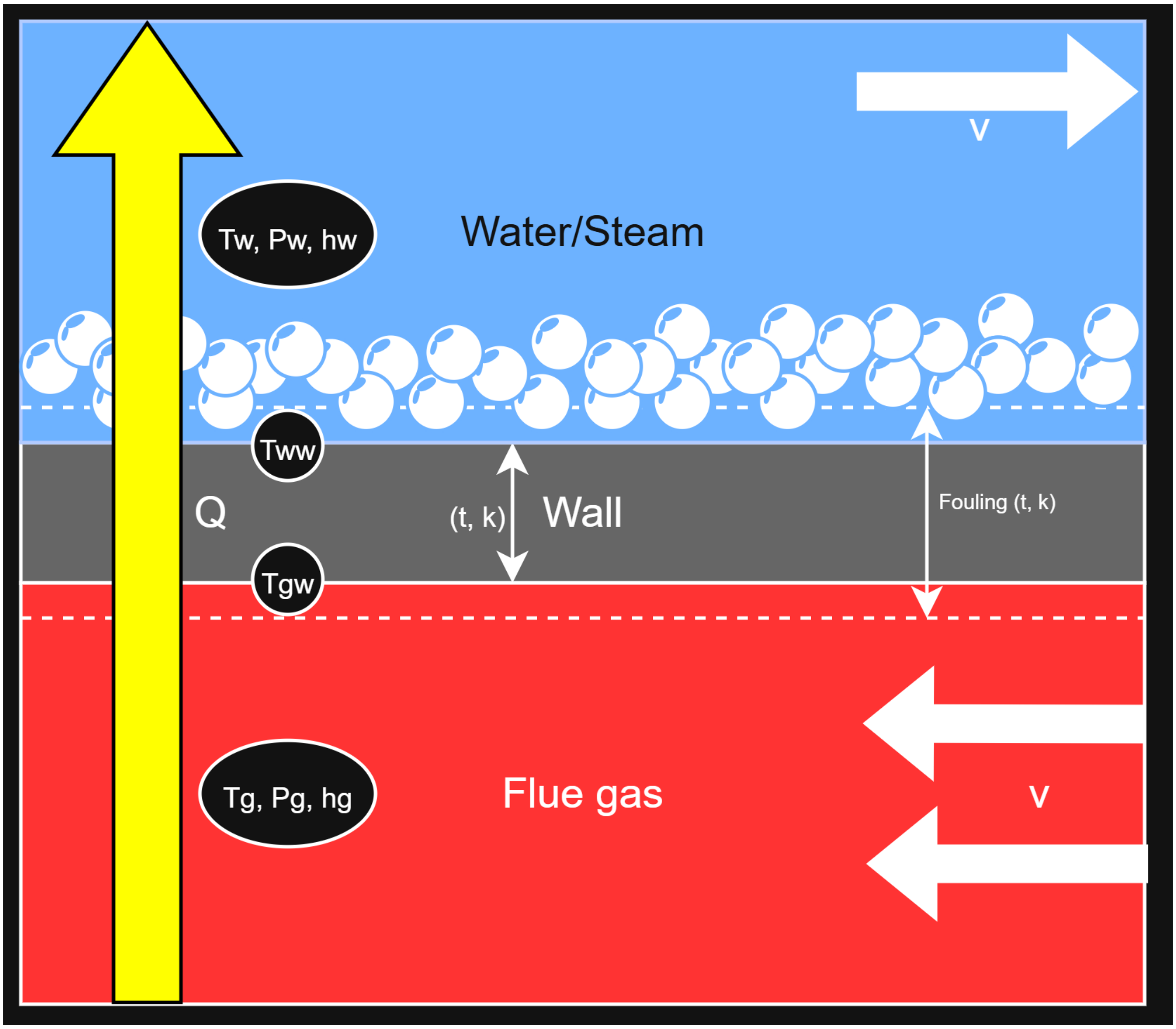

Figure 5.1: Cross section of heat transfer network from gas to water/steam

5.2 Local energy balance

For each differential segment of length dx, the model enforces a one-dimensional steady-state energy balance between the gas, the water and the tube wall:

- Heat transferred across the wall:

$$q'(x) = UA'(x)\left[T_g(x) - T_w(x)\right]$$

- Relation to the segment duty:

$$\mathrm{d}Q(x) = q'(x)\,\mathrm{d}x$$

- Gas stream:

$$\mathsf{d}Q(x) = -\,\dot{m}_g\,\mathsf{d}h_g(x) \quad \Rightarrow \quad \frac{\mathsf{d}h_g}{\mathsf{d}x} = -\,\frac{q'(x)}{\dot{m}_g}$$

- Water stream:

$$\mathsf{d}Q(x) = +\,\dot{m}_w\,\mathsf{d}h_w(x) \quad \Rightarrow \quad \frac{\mathsf{d}h_w}{\mathsf{d}x} = +\,\frac{q'(x)}{\dot{m}_w}$$

In the numerical implementation these equations are applied in finite-difference form over each marching step:

$$Q_{\text{step}} = q'(x)\,\Delta x$$

$$\Delta h_g = -\frac{Q_{\text{step}}}{\dot{m}_g}, \qquad \Delta h_w = +\frac{Q_{\text{step}}}{\dot{m}_w}$$

5.3 Overall conductance and resistance network

The overall conductance per unit length $UA'(x)$ is obtained from a radial series of thermal resistances per unit length:

- Gas-side convection:

$$R'_g = \frac{1}{h_g(x)\,P_g}$$

- Gas-side fouling:

$$R'_{fg} = R'_{fi}(P_g) \quad \text{(from specified fouling thickness and conductivity)}$$

- Tube wall:

$$R'_w = \frac{\mathsf{ln}\big(D_o/D_i\big)}{2\pi k_w}$$

- Water-side fouling:

$$R'_{fc} = R'_{fo}(P_w)$$

- Water-side convection:

$$R'_c = \frac{1}{h_w(x)\,P_w}$$

where D_i and D_o are the tube inner and outer diameters and k_w is the tube wall thermal conductivity. Combining these contributions:

$$\frac{1}{UA'(x)} = R'_g + R'_{fg} + R'_w + R'_{fc} + R'_c$$

or equivalently,

$$UA'(x) = \left[\frac{1}{h_g P_g} + R'_{fg} + R'_w + R'_{fc} + \frac{1}{h_w P_w}\right]^{-1}$$

The linear heat flux then follows directly:

$$q'(x) = UA'(x)\left[T_g(x) - T_w(x)\right]$$

5.4 Wall temperature update and thermal convergence

The tube wall temperatures on the gas and water sides, T_{gw} and T_{ww}, are updated using a two node wall model in each marching step.

Given $q'(x)$, the wall side energy balances yield:

$$T_{gw} = T_g - \frac{q'}{h_{g,\text{tot}}}$$

$$T_{ww} = T_w + \frac{q'}{h_w}$$

The wall conduction temperature drop is:

$$\Delta T_{\text{wall}} = T_{gw} - T_{ww}$$

which is also equal to:

$$\Delta T_{\text{wall}} = q'\left[R'_{fg} + R'_w + R'_{fc}\right]$$

A consistency check is applied; if the implied wall temperature difference from conduction differs from the one implied by convection, the marching solver iterates the HTC evaluation once with relaxed updates (default under-relaxation factor 0.35).

In the actual implementation this consistency check is performed by iterating on T_{gw}, T_{ww}, and q' using the full resistance network (gas convection, gas fouling, wall, water fouling, water convection), with an under-relaxation factor applied to both wall temperatures and the linear heat flux.

If temperature overshoot (negative film coefficient, reversed driving force) is detected within a step, the step is automatically halved and recomputed.

5.5 Stage and boiler level duties

For a stage of length L_j, the stage heat duty and stage level conductance are obtained by integrating the local quantities along x:

$$Q_{\text{stage},j} = \int_0^{L_j} q'(x)\,\mathsf{d}x \approx \sum_i q'_i\,\Delta x_i$$

$$(UA)_j = \int_0^{L_j} UA'(x)\,\mathsf{d}x \approx \sum_i UA'_i\,\Delta x_i$$

The total useful boiler duty is the sum of all stage duties:

$$Q_{\text{useful}} = \sum_{j=1}^{6} Q_{\text{stage},j}$$

These integrated quantities are later used in the performance and efficiency evaluation (Section 7) and for constructing stage-wise summary tables.

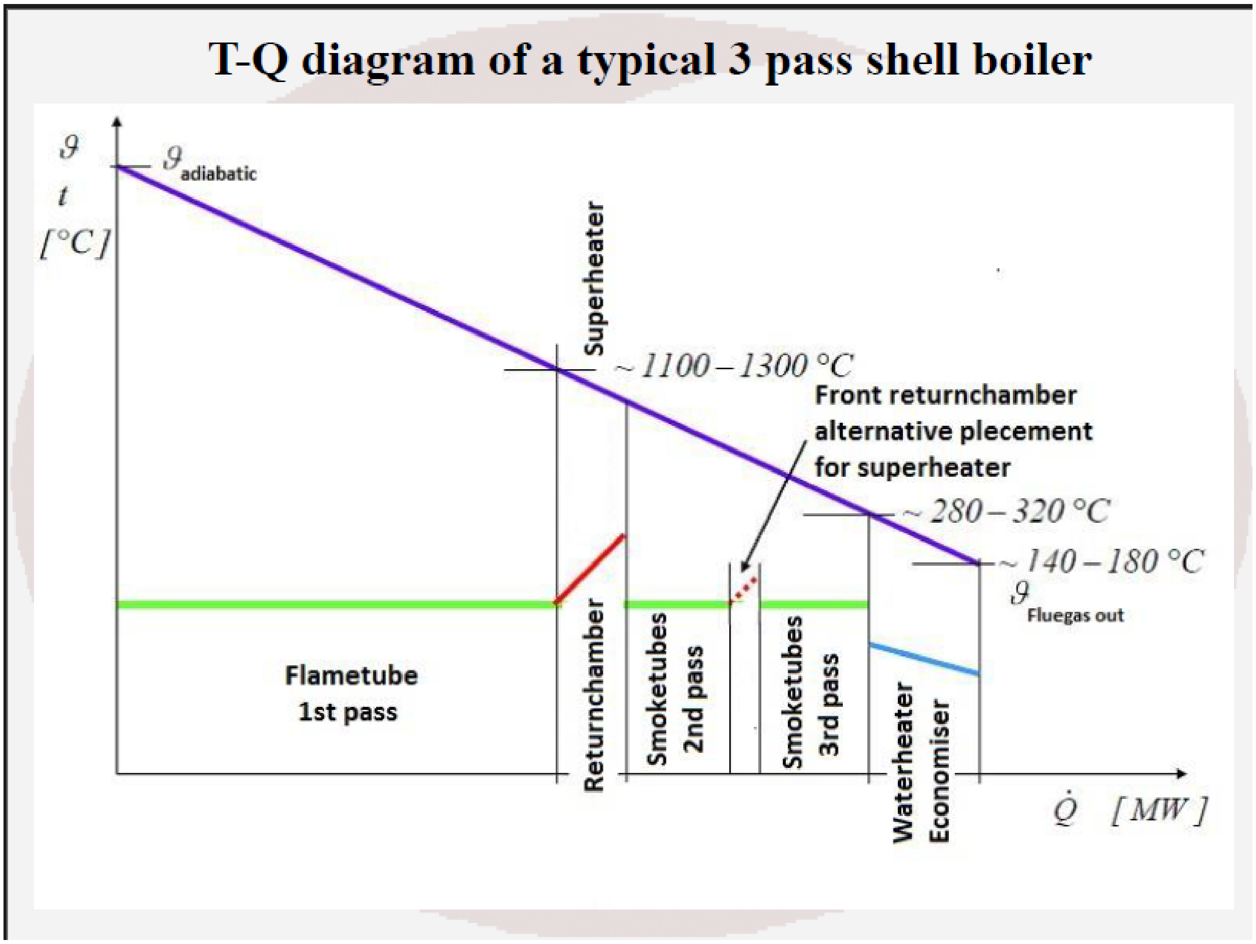

Figure 5.2: Representative T–Q diagram for the three-pass boiler, showing gas and water/steam temperature evolution and stage heat duties HX$_1$–HX$_6$.

5.6 Gas side

Gas side heat transfer is computed with geometry aware correlations based on local gas properties from Cantera (`GasProps`) and stage specific geometry from the `GeometryBuilder`. For each marching step, the total gas side HTC is split into a convective and a radiative contribution:

$$h_{g,\text{tot}} = h_{g,\text{conv}} + h_{g,\text{rad}}$$

The implementation uses the helper `gas_htc_parts(g, spec, T_{gw})`, which returns $(h_{g,\text{conv}}, h_{g,\text{rad}})$ in W/m²·K, and then sums them in `gas_htc`.

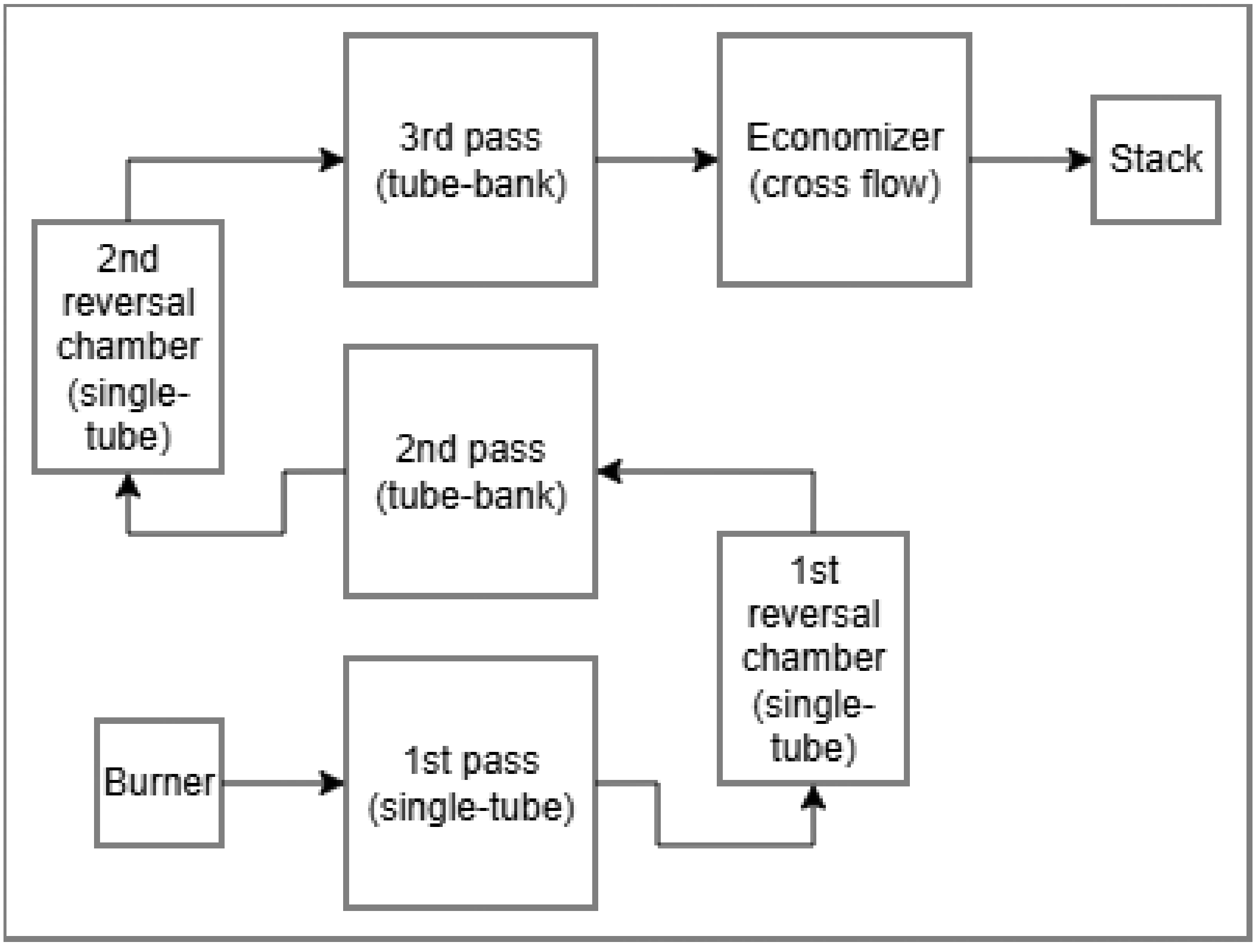

Figure 5.3: Path of flue gas through the 6 stages

5.6.1 Single tube and reversal chamber

Stages of kind `single_tube` and `reversal_chamber`, corresponding to furnace (first pass), and both reversal chambers, are treated as internal forced convection in a circular duct. The characteristic quantities are:

- Diameter: D (supplied by `stages.yaml`)
- Length: L (supplied by `stages.yaml`)
- Flow area: $A = \frac{1}{4} pi\, D^2$ (calculated by geometry builder)
- Velocity:

$$V = \frac{\dot{m}_g}{\rho_g A}$$

- Reynolds and Prandtl numbers:

$$\text{Re} = \frac{\rho_g V D}{\mu_g}, \qquad \text{Pr} = \frac{c_{p,g}\, \mu_g}{k_g}$$

Local gas properties $\rho_g, \mu_g, k_g, c_{p,g}$ are obtained from the Cantera mixture via the functions defined in `common\props.py`, at the local gas temperature and pressure. (McBride et al. 1993)

Laminar/developing flow (Graetz-type)

For Re < 2300, uses a Graetz correlation for thermally developing laminar flow:

$$\mathrm{Gz} = \mathrm{Re}\,\mathrm{Pr}\,\frac{D}{L}$$

$$\mathrm{Nu} = 3.66 \;+\; \frac{0.0668\,\mathrm{Gz}}{1 + 0.04\,\mathrm{Gz}^{2/3}}$$

(Incropera et al. 2011)

Turbulent flow (Gnielinski with Petukhov friction factor)

For Re ≥ 2300, the Gnielinski correlation is applied with a Petukhov friction factor:

$$f = \left(0.79\,\ln\mathrm{Re} - 1.64\right)^{-2}$$

(Munson et al. 2013)

$$\mathrm{Nu} = \frac{\frac{f}{8}(\mathrm{Re} - 1000)\,\mathrm{Pr}}{1 + 12.7\,\sqrt{\frac{f}{8}}\left(\mathrm{Pr}^{2/3} - 1\right)}$$

(Incropera et al. 2011) The local convective heat-transfer coefficient is then:

$$h_{g,\mathrm{conv}} = \frac{\mathrm{Nu}\,k_g}{D}$$

(Incropera et al. 2011)

This same internal correlation is used for `single_tube`, `reversal_chamber` and `tube_bank` gas-side flow (see below).

5.6.2 Tube bank

Stages `tube_bank` correspond to tube bundles inside the shell, ie. first and second passes. In this model, the gas side is still treated as internal flow inside the tubes:

- Hot side (gas): inside tubes (inner diameter D_i), using the same internal forced convection model as in Section 5.2.1.

Thus the gas side convective HTC in tube-bank stages is:

$$h_{g,\text{conv}}^{(\text{HX3,5})} = \frac{\text{Nu}(\text{Re}, \text{Pr})\, k_g}{D_i}$$

with Nu given by the Graetz/Gnielinski formulation above, and Re, Pr computed from the local gas properties and tube hydraulic diameter.

5.6.3 Economizer

The economizer `economiser` stage reverses the roles: gas flows outside the tubes in cross flow, while water flows inside. The gas side convection is then modelled as external cross flow over a tube bank.

Key geometry quantities (from `GeometryBuilder` for the economizer):

- Tube outer diameter: $D = D_o$
- Gas side cross flow area: $A_{\text{bulk}} = A_{\text{hot,flow}}$
- Optional maximum/mean velocity factor:

$$V_{\text{bulk}} = \frac{\dot{m}_g}{\rho_g A_{\text{bulk}}}, \qquad V = u_{\text{max}} V_{\text{bulk}}$$

  where u_{max} is calculated depending on the tube bank arrangement and spacing between tubes.

- Reynolds and Prandtl numbers:

$$\text{Re} = \frac{\rho_g V D}{\mu_g}, \qquad \text{Pr} = \frac{c_{p,g}\, \mu_g}{k_g}$$

For `”economiser”` stages the primary correlation is a banded Zukauskas form for cross flow over tube banks:

$$\text{Nu} = C\, \text{Re}^m\, \text{Pr}^n$$

(Incropera et al. 2011)

where the coefficients C, m are selected from standard bands as a function of Reynolds number and tube arrangement (`inline` vs `staggered`), and the exponent n is:

$$n = \begin{cases} 0.36, & \text{Pr} \leq 10 \\ 0.25, & \text{Pr} > 10 \end{cases}$$

If Re falls outside the tabulated bands, the model falls back to the Churchill–Bernstein correlation for cross flow over a single cylinder:

$$\text{Nu} = 0.3 \; + \; \frac{0.62\,\text{Re}^{1/2}\,\text{Pr}^{1/3}}{\left[1 + (0.4/\text{Pr})^{2/3}\right]^{1/4}} \left[1 + \left(\frac{\text{Re}}{282000}\right)^{5/8}\right]^{4/5}$$

(Incropera et al. 2011) The gas-side convective HTC in the economizer is then:

$$h_{g,\text{conv}}^{\text{(HX6)}} = \frac{\text{Nu}\,k_g}{D_o}$$

(Incropera et al. 2011)

5.6.4 Radiation model

Radiative heat transfer from the flue gas to the furnace surfaces is explicitly accounted for by a participating medium model for the H_2O/CO_2 mixture. The implementation follows a simplified Smith–Shen–Friedman style four gray model.

For each step, the gas emissivity is computed as:

1. Partial pressures of participating species:

   $$p_{\text{H}_2\text{O}} = y_{\text{H}_2\text{O}}\,P, \qquad p_{\text{CO}_2} = y_{\text{CO}_2}\,P$$

   (Modest 2013) where y_i are molar (or mass-fraction-equivalent) composition entries from the flue gas stream, and P is the local gas pressure.

2. Mean beam length:

   $$L_b = \begin{cases} L_{\text{rad,override}}, & \text{if specified in the stage} \\ 0.9\,D_{h,\text{gas}}, & \text{otherwise} \end{cases}$$

   (Modest 2013) with $D_{h,\text{gas}}$ the gas-side hydraulic diameter.

3. Effective optical thickness in each gray band:

$$p_{\text{ratio}} = \frac{p_{\text{H}_2\text{O}} + p_{\text{CO}_2}}{P_{\text{atm}}}$$

   (Modest 2013)

$$\tau_j = K_j \left(\frac{T}{1000\,\text{K}} \right)^{T_{\text{exp}}} p_{\text{ratio}}\, L_b$$

   (Modest 2013)

   where K_j and weighting factors A_j are fixed band coefficients, T is the gas temperature, and T_{exp} is a temperature exponent (default 0.65, configurable per stage via `rad_Texp`).

4. Total gas emissivity:

$$\varepsilon_g = 1 - \sum_{j=1}^{4} A_j \, \text{exp}(-\tau_j)$$

   (Modest 2013) with ε_g constrained to $[0, 1]$.

A mean-film temperature is used for the linearized radiative HTC:

$$T_{\text{film}} = \frac{T_g + T_{gw}}{2}$$

$$h_{g,\text{rad}} = 4\,\sigma\,F\,\varepsilon_g\,T_{\text{film}}^3$$

(Modest 2013)

where:

- σ is the Stefan–Boltzmann constant,
- F is an effective view factor (default 1.0 or stage-specific `rad_F`).

The gas-side total HTC reported and used in the resistance network is then:

$$h_{g,\text{tot}} = h_{g,\text{conv}} + h_{g,\text{rad}}$$

and the corresponding convective/radiative contributions to the linear heat flux are tracked via:

$$q'_{\text{conv}} = q' \, \frac{h_{g,\text{conv}}}{h_{g,\text{tot}}}, \qquad q'_{\text{rad}} = q' - q'_{\text{conv}}$$

These diagnostics are later integrated on a per-stage basis to quantify the share of convective vs radiative heat transfer in each section of the boiler.

5.7 Water side

Water side heat transfer is computed with geometry dependent correlations using local water properties from IAPWS97 (`WaterProps`), with stage specific geometry from the `GeometryBuilder`. The solver always works with a single effective water side heat transfer coefficient $h_w(x)$ per marching step, which may represent:

- pure pool boiling at a saturated surface,
- a Chen type combination of forced convection and nucleate boiling, or
- single phase forced convection.

In the implementation this logic is encapsulated in `water_htc`, which returns (h_w) for each step.

5.7.1 General formulation and boiling treatment

The six stages of the boiler are divided, from the water-side point of view, into:

- HX$_1$–HX$_5$: pool-boiling stages
  (`pool_boiling = true` in the stage specification)
- HX$_6$: economizer stage
  (`pool_boiling = false`)

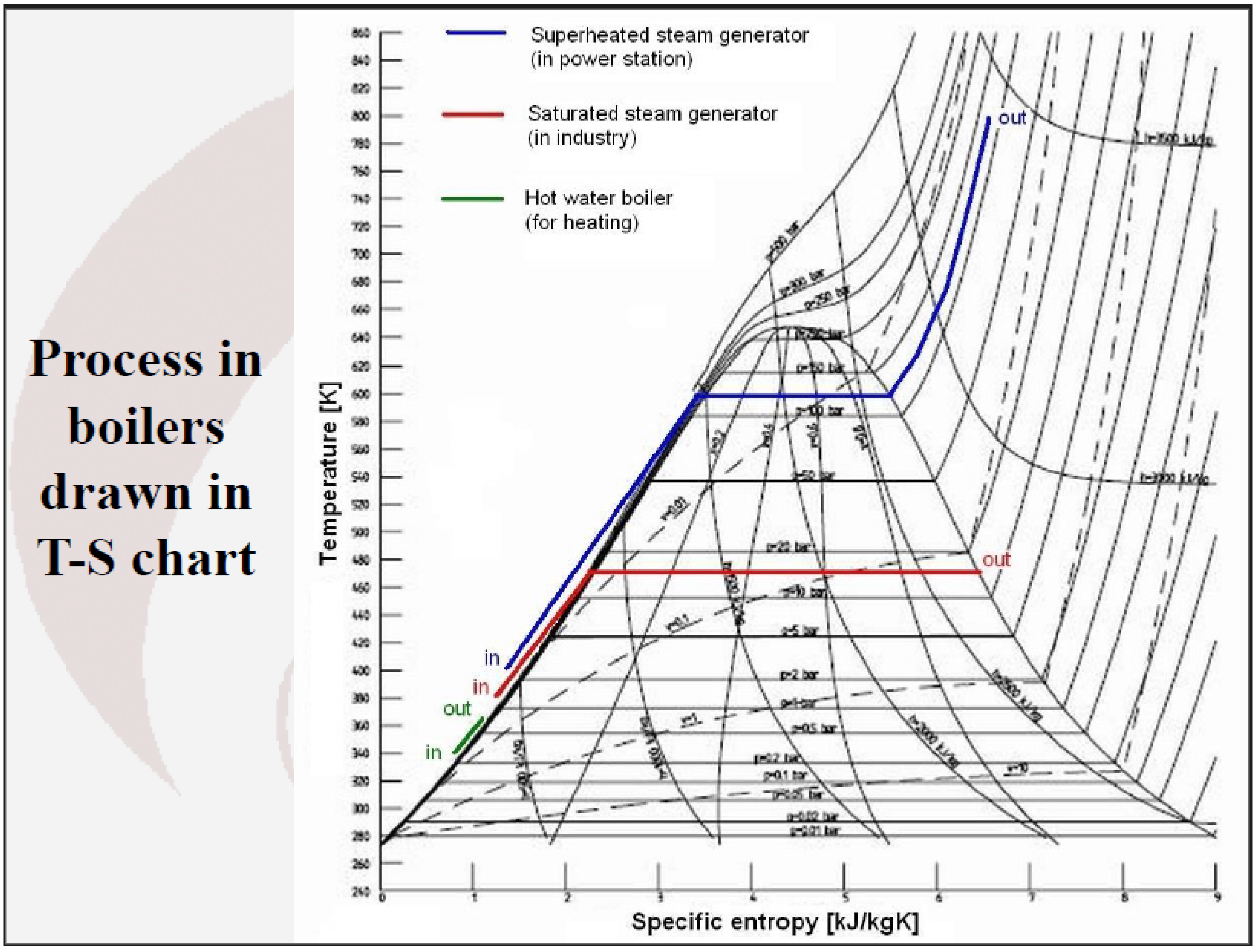

Figure 5.4: Temperature–entropy (T–s) representation of the feedwater heating and evaporation process across economiser and boiler at the operating pressure.

The solver applies the following decision tree at each marching step:

1. Pool-boiling stages (HX$_1$–HX$_5$)

   If the stage is flagged as `pool_boiling = true`, the bulk water temperature entering the wall-energy balance is fixed at the saturation temperature at the local pressure:

$$T_w = T_{\text{sat}}(p_w),$$

   and the water-side HTC is computed from the Cooper pool boiling correlation for nucleate boiling correlation:

$$h_{\text{Cooper}} = 55\, p_r^{0.12-0.2\,\log_{10}(R_p)} \left[-\log_{10}(p_r)\right]^{-0.55} q''^{0.67}$$

   where

$p_r = \dfrac{p}{p_{\text{crit}}} =$ reduced pressure, $\quad R_p =$ surface roughness (μm), $\quad q'' =$ heat flux.

(Incropera et al. 2011)

This nucleate-boiling HTC is then used directly:

$$h_w = h_{w,\text{nb}},$$

and the step is always marked as boiling in the post processing.

In other words, the main boiling surfaces of the boiler (furnace, passes, reversal chambers) are represented as heated surfaces in a saturated pool, with the HTC governed by the local heat flux and surface roughness rather than by a detailed prediction of liquid velocity. This matches the natural circulation character of these sections.

2. Non pool boiling stages (HX$_6$, economizer)

For stages with `pool_boiling = false`, the model can represent both single phase convection and flow boiling via a Chen type formulation.

a. Boiling detection

A helper determines whether the local state is boiling based on the bulk enthalpy h and, when needed, the wall temperature T_{wall}:

- if
$$h_f(p_w) \leq h \leq h_g(p_w)$$
the state is inside the saturation interval and is treated as two phase;
- if $h < h_f(p_w)$ (slightly subcooled liquid) but the wall superheat is sufficiently high,
$$T_{\text{wall}} > T_{\text{sat}}(p_w) + \Delta T_{\text{crit}},$$
the state is also treated as boiling;
- otherwise the flow is treated as single-phase liquid.

Here h_f and h_g are saturated-liquid and saturated vapor enthalpies at the local pressure, obtained via IAPWS97.

b. Single-phase regime

If boiling is not detected, the water side HTC is purely convective:

$$h_w = h_{w,\text{conv}},$$

with $h_{w,\text{conv}}$ obtained from a geometry dependent forced convection correlation (internal tube, external tube bank, or external single tube/bend) as detailed in Sections [5.7.2]–[5.7.4].

c. Flow boiling regime (Chen model)

When boiling is detected in a non pool boiling stage, the HTC is constructed as a Chen type superposition of:

- a liquid only convective term h_{lo}, and
- a nucleate-boiling term h_{nb} using the same Cooper correlation as in pool boiling.

The liquid only HTC is evaluated at the saturation temperature $T_{\text{sat}}(p)$ and using the appropriate geometry correlation:

$$h_{\text{lo}} = h_{\text{single-phase}}\big(T_{\text{sat}}(p), \text{geometry}\big),$$

while the nucleate-boiling term is

$$h_{\text{nb}} = h_{\text{Cooper}}(p, q'').$$

The Chen combination used in the code is:

$$h_w = F\,h_{\text{lo}} + S\,h_{\text{nb}}.$$

(Incropera et al. 2011)

The convection enhancement factor F is based on a Martinelli type parameter X_{tt},

$$X_{tt} = \left(\frac{1-x}{x}\right)^{0.9}\left(\frac{\mu_l}{\mu_g}\right)^{0.1}\left(\frac{\rho_g}{\rho_l}\right)^{0.5},$$

where x is the local vapor quality and $\rho_l, \rho_g, \mu_l, \mu_g$ are liquid/vapor densities and viscosities at saturation. A bounded form of the Chen factor is then used:

$$F = 1 + 0.12\,X_{tt}^{-0.8},$$

The suppression factor S modulating the nucleate boiling contribution is a function of mass flux and Reynolds number:

$$S = \frac{1}{1 + C\,\text{Re}_{\text{lo}}^{\alpha}},$$

where Re_{lo} is a liquid only Reynolds number based on the mass flux

$$G = \frac{\dot{m}_w}{A_{\text{flow}}},$$

and the liquid properties at saturation. In the implementation the constants and bounds are chosen such that S remains between about 0.1 and 1.0, reducing the nucleate boiling influence at very high mass flux (strong forced convection).

In the present thesis this Chen type flow boiling capability is only exercised in the economizer stage; the main boiling sections (HX_1–HX_5) use the pure pool boiling representation above.

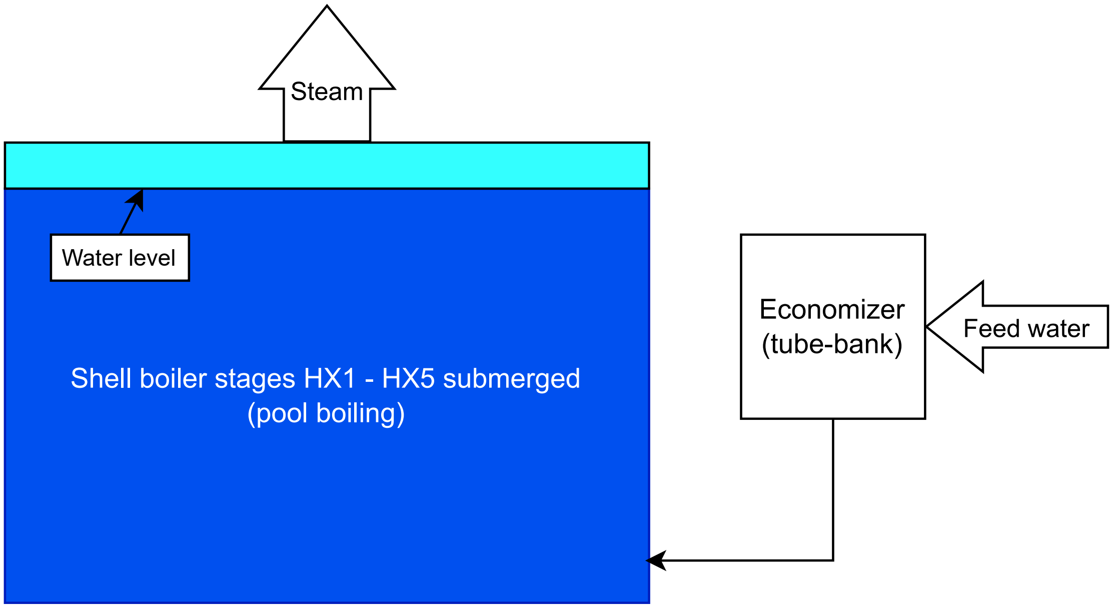

Figure 5.5: Path of water/steam through the 6 stages

5.7.2 Economizer

In the economizer stage (HX_6, `kind = ”economiser”`), water flows inside the tubes and is heated by the flue gas flowing externally in cross flow. This stage is the only one where `pool_boiling = false` and where the full single phase/Chen type boiling formulation is used.

Velocity and dimensionless groups

The relevant geometric quantities for the water side are:

- tube inner diameter: D_i,
- tube length: L,

- cold-side flow area: $A_{\text{cold,flow}}$.

The bulk water velocity, Reynolds and Prandtl numbers are:

$$V_w = \frac{\dot{m}_w}{\rho_w A_{\text{cold,flow}}},$$

$$\text{Re}_w = \frac{\rho_w V_w D_i}{\mu_w}, \qquad \text{Pr}_w = \frac{c_{p,w}\,\mu_w}{k_w},$$

with $\rho_w, \mu_w, k_w, c_{p,w}$ evaluated from IAPWS97 at the film temperature. (Wagner and Pruss 1997)

Single phase internal flow correlation

When no boiling is detected in the economizer, the Nusselt number is computed using a Gnielinski type internal flow correlation with a viscosity ratio correction:

- Laminar / developing regime (Re$_w < 2300$): a Graetz type form is used

$$\text{Gz}_w = \text{Re}_w\,\text{Pr}_w\,\frac{D_i}{L},$$

$$\text{Nu}_w = 3.66 + \frac{0.0668\,\text{Gz}_w}{1 + 0.04\,\text{Gz}_w^{2/3}}.$$

- Turbulent regime (Re_$w \geq 2300$): Gnielinski correlation with friction factor

$$f_w = \left(0.79\,\text{ln}\,\text{Re}_w - 1.64\right)^{-2},$$

(Munson et al. 2013)

$$\text{Nu}_w = \frac{\frac{f_w}{8}(\text{Re}_w - 1000)\,\text{Pr}_w}{1 + 12.7\sqrt{\frac{f_w}{8}}\left(\text{Pr}_w^{2/3} - 1\right)},$$

(Incropera et al. 2011) scaled by a viscosity-ratio correction:

$$\text{Nu}_w \leftarrow \text{Nu}_w \left(\frac{\mu_b}{\mu_w}\right)^{0.11},$$

where μ_b is evaluated at the bulk temperature and μ_w at the wall temperature.

The single phase water side HTC in the economizer is then:

$$h_{w,\text{conv}}^{\text{(HX6)}} = \frac{\text{Nu}_w \, k_w}{D_i}.$$

(Incropera et al. 2011)

Flow boiling in the economizer

If boiling is detected in the economizer (according to the criteria in the general formulation), the same geometry and mass flux information are used to form the liquid only HTC h_{lo} and the Cooper nucleate boiling HTC h_{nb}. The total water side HTC is then:

$$h_w = F \, h_{\text{lo}} + S \, h_{\text{nb}},$$

with F and S given by the Chen type relations described above, using the local vapor quality, mass flux, and saturation properties. This provides a smooth transition between predominantly convective and predominantly nucleate boiling regimes in the economizer.

5.7.3 Tube bank stages

For completeness, the water side model also includes correlations for cross flow over tube banks on the cold side (`kind = ”tube_bank”`), although in the present thesis these stages are operated in pool boiling mode (so that only the Cooper correlation is used). When a tube bank description is required on the water side, the geometry is:

- tube outer diameter: D_o,
- cold-side flow area: $A_{\text{cold,flow}}$,
- number of rows: N_{rows},
- transverse and longitudinal pitches: S_T, S_L,
- bundle arrangement: `inline` or `staggered`.

The water velocity, Reynolds and Prandtl numbers are:

$$V_w = \frac{\dot{m}_w}{\rho_w A_{\text{cold,flow}}},$$

$$\text{Re}_w = \frac{\rho_w V_w D_o}{\mu_w}, \qquad \text{Pr}_w = \frac{c_{p,w} \, \mu_w}{k_w}.$$

A Zukauskas-type banded correlation is then applied:

$$\text{Nu}_w = C \, \text{Re}_w^m \, \text{Pr}_w^n,$$

(Incropera et al. 2011) where:

- C, m are selected from standard Zukauskas bands based on Re_w and the arrangement (`inline` or `staggered`),
- the exponent n is

$$n = \begin{cases} 0.36, & \mathrm{Pr}_w \le 10 \\ 0.25, & \mathrm{Pr}_w > 10 \end{cases}$$

The raw Nusselt number is further modified by:

- a row factor $f_{\mathrm{row}}(N_{\mathrm{rows}})$ that accounts for the finite number of tube rows, and
- a spacing factor $\phi(S_T, S_L, D_o)$ that accounts for maximum velocity effects in the tube bank (greater constriction $\Rightarrow$ higher HTC).

If Re_w falls outside the Zukauskas validity range, the model falls back to the Churchill Bernstein correlation for cross flow over a single cylinder:

$$\mathrm{Nu}_w = 0.3 + \frac{0.62\,\mathrm{Re}_w^{1/2}\,\mathrm{Pr}_w^{1/3}}{\left[1 + (0.4/\mathrm{Pr}_w)^{2/3}\right]^{1/4}} \left[1 + \left(\frac{\mathrm{Re}_w}{282000}\right)^{5/8}\right]^{4/5}.$$

(Incropera et al. 2011)

The corresponding water side HTC for a tube-bank configuration is:

$$h_{w,\mathrm{conv}}^{(\mathrm{bank})} = \frac{\mathrm{Nu}_w\, k_w}{D_o}.$$

(Incropera et al. 2011)

When such a tube bank model is used inside the Chen formulation, h_{lo} is taken from this $h_{w,\mathrm{conv}}^{(\mathrm{bank})}$.

5.7.4 Single tube and reversal chamber stages

Stages of kind `single_tube` and `reversal_chamber` correspond, on the water side, to external flow around one or more tubes within the drum/shell region. In the current thesis these are also operated in pool boiling mode (`pool_boiling = true`), so the Cooper pool boiling correlation described in the general formulation dominates their behavior. Nevertheless, the implementation includes external forced convection correlations for completeness.

For these stages the characteristic length for the water side is the tube outer diameter D_o, and the cold side flow area $A_{\mathrm{cold,flow}}$ is defined by the drum cross section minus the tube area(s). When a cross flow description is used for single-phase or liquid only HTC:

- water velocity, Reynolds and Prandtl numbers:

$$V_w = \frac{\dot{m}_w}{\rho_w A_{\text{cold,flow}}},$$

$$\mathsf{Re}_w = \frac{\rho_w V_w D_o}{\mu_w}, \qquad \mathsf{Pr}_w = \frac{c_{p,w}\,\mu_w}{k_w}.$$

For a single tube in cross flow (or, by approximation, a relatively open bundle) a Churchill Bernstein style correlation is used:

$$\mathsf{Nu}_w = 0.3 + \frac{0.62\,\mathsf{Re}_w^{1/2}\,\mathsf{Pr}_w^{1/3}}{\left[1 + (0.4/\mathsf{Pr}_w)^{2/3}\right]^{1/4}} \left[1 + \left(\frac{\mathsf{Re}_w}{282000}\right)^{5/8}\right]^{4/5},$$

(Incropera et al. 2011) leading to

$$h_{w,\text{conv}}^{(\text{single})} = \frac{\mathsf{Nu}_w\,k_w}{D_o}.$$

In reversal chamber segments, the tubes are bent, and the model applies the same base correlation multiplied by a curvature (bend) factor:

$$h_{w,\text{conv}}^{(\text{rev})} = \phi_{\text{bend}}(D_o, R_c)\,\frac{\mathsf{Nu}_w\,k_w}{D_o},$$

where R_c is the bend radius and $\phi_{\text{bend}} \geq 1$ is a modest enhancement (up to roughly 1.25) for tight bends, reflecting locally increased turbulence around the bend region.

In pool boiling operation these external convection correlations are only used implicitly inside the liquid only component h_{lo} when the Chen type formulation is invoked. For the main boiling sections in this thesis, however, the water side is predominantly controlled by the Cooper pool boiling correlation with $T_w = T_{\text{sat}}(p)$.

Chapter 6

Hydraulic Model

Hydraulic behavior is extracted directly from the solver through the per step pressure drop decomposition implemented in `heat/solver.py` (`_gas_dp_components`, `pressure_drop_gas`) and accumulated at the stage level in `heat/solver.py::solve_stage`.

The model divides gas side pressure losses into:

- Frictional losses
- Minor losses (inlet, outlet, bends, etc.)
- Total pressure drop (sum of the above)

Water side pressure losses are intentionally not included in this model (water is taken at constant drum pressure).

6.1 Frictional losses

The per step frictional pressure drop follows a standard 1D formulation:

$$\Delta P_{\text{fric}} = -f\,\frac{\Delta x}{D_h}\left(\frac{\rho V^2}{2}\right)$$

(White 2016)

Here:

- f is the Darcy friction factor,
- D_h is the gas side hydraulic diameter (`hot_Dh`),
- ρ and V are local gas density and velocity,
- Δx is the current marching step length.

The friction factor is computed from Reynolds number and relative roughness via `_friction_factor`:

- Laminar (Re < 2300):

  $$f = \frac{64}{\text{Re}}$$

  (White 2016)

- Transitional ($2300 \leq$ Re < 4000): linear blend between laminar and turbulent values:

  $$f = (1 - w) f_{\text{lam}} + w f_{\text{turb}}, \quad w = \frac{\text{Re} - 2300}{4000 - 2300}$$

  (Crane Co. 2018)

- Turbulent (Re ≥ 4000):
  Colebrook–White is solved iteratively, seeded by the Swamee–Jain explicit approximation.

  Swamee–Jain seed (used as the initial guess):

  $$f_{\text{SJ}} = \frac{0.25}{\left[\log_{10}\left(\frac{\varepsilon/D_h}{3.7} + \frac{5.74}{\text{Re}^{0.9}}\right)\right]^2}$$

  (Swamee and Jain 1976)

  Colebrook–White equation solved iteratively in the code:

  $$\frac{1}{\sqrt{f}} = -2 \, \log_{10}\left(\frac{\varepsilon/D_h}{3.7} + \frac{2.51}{\text{Re}\sqrt{f}}\right)$$

  (White 2016)

  The iteration is performed on $1/\sqrt{f}$ until convergence.

6.2 Minor losses

Minor losses are applied using per–stage catalogue K values. For each stage, a total loss coefficient K_{sum} is assembled from geometry and user inputs:

- `economiser`
  Minor losses are neglected:

  $$K_{\text{sum}} = 0$$

- `reversal_chamber`
  Includes nozzle and bend losses:
  - Inlet/outlet: `nozzle_k_in` + `nozzle_k_out` (if provided),
  - Bend loss K_{bend} based on curvature ratio:

  $$K_{\text{bend}} = R_c / D_o$$

    with a fallback $K_{\text{bend}} = 0.5$ if geometry is missing.
- `single_tube`
  Defaults are used if not overridden in the spec:

  $$K_{\text{contraction}} = 0.5, \quad K_{\text{expansion}} = 1.0, \quad K_{\text{exit}} = 1.0$$

  so that

  $$K_{\text{sum}} = K_{\text{contraction}} + K_{\text{expansion}} + K_{\text{exit}}$$
- `tube_bank`
  Defaults to zero for all minor loss coefficients unless explicitly provided:

  $$K_{\text{contraction}},\ K_{\text{expansion}},\ K_{\text{exit}} \to 0$$

Once K_{sum} is known, it is uniformly distributed over the N marching steps of that stage:

Minor-loss pressure drop is given by:

$$\Delta P_{\text{minor}} = K \left(\frac{\rho V^2}{2} \right)$$

(Crane Co. 2018)

$$K_{\text{per step}} = \frac{K_{\text{sum}}}{N}$$

The per–step minor loss is then

$$\Delta P_{\text{minor}} = -K_{\text{per step}} \left(\frac{\rho V^2}{2} \right)$$

6.3 Total gas side pressure drop

For each step, the total gas–side pressure change is the sum of frictional and minor components:

$$\Delta P_{\text{total}} = \Delta P_{\text{fric}} + \Delta P_{\text{minor}}$$

(White 2016)

This is what `pressure_drop_gas` returns and what is applied to the gas stream in `update_gas_after_step`.

6.4 Coupling of ΔP into the energy solver

Gas pressure is updated step–wise using the same ΔP model:

$$P_{i+1} = P_i + \Delta P_{\text{total}}(P_i, T_i, \dots)$$

After each step:

1. The local gas state $(T_i, P_i, \text{composition})$ is used to evaluate ρ, μ, k, and c_p.
2. The friction factor and dynamic pressure are computed from these properties.
3. ΔP_{fric} and ΔP_{minor} are formed.
4. The updated pressure P_{i+1} is used for the next step, so density, viscosity, Reynolds number, and gas side HTC h_g are all evaluated at the updated pressure.

In this way, compressibility enters through the pressure dependence of $\rho(T, P)$ and $\mu(T, P)$ and their effect on V, Re, and f.

Chapter 7

Performance

This section summarizes the boiler level performance obtained from the coupled combustion heat transfer simulation. All numerical values are extracted from the stages summary and boiler summary data produced by the post-processing step `heat/postproc.py`.

7.1 solution procedure

For any given operating conditions, the main solver `run_boiler_case()` performs an outer fixed point iteration, on boiler efficiency, and water mass flow:

1. The combustion sub-model called by `Combustor.run()`, returns:
   - the lower heating value based firing rate P_{LHV},
   - the total combustion heat release Q_{in},
   - the adiabatic flame temperature T_{ad},
   - the fully burnt flue-gas stream at burner exit.
2. Given a current efficiency guess $\eta^{(n)}$ and the combustion result, the corresponding feedwater/steam mass flow $\dot{m}_w^{(n)}$ is computed by `_water_mass_from_efficiency()` as

$$h_{\text{in}} = h_{\text{fw}}(P_{\text{fw}}), \qquad h_{\text{steam}} = h_g(P_{\text{fw}}),$$

$$\Delta h = h_{\text{steam}} - h_{\text{in}},$$

$$Q_{\text{target}}^{(n)} = \eta^{(n)}\, Q_{\text{in}},$$

$$\dot{m}_w^{(n)} = \frac{Q_{\text{target}}^{(n)}}{\Delta h}.$$

3. A `WaterStream` with mass flow $\dot{m}_w^{(n)}$ is created and passed, together with the combustion flue gas `GasStream` and the drum/stage definitions, to the multi stage heat exchanger solver `run_hx()`.
4. `run_hx()` returns per stage and boiler level summary tables.
5. The new efficiency estimate is set to the indirect efficiency,

$$\eta^{(n+1)} := \eta_{\text{indirect}}^{(n)},$$

And the procedure is repeated until the change in water mass flow between iterations is below the specified tolerance

$$\left|\dot{m}_w^{(n)} - \dot{m}_w^{(n-1)}\right| < 10^{-3}\,\text{kg/s},$$

or a maximum number of iterations is reached.

At convergence, returning:

- converged water/steam mass flow $\dot{m}_{w,\text{base}}$,
- converged indirect efficiency $\eta_{\text{indirect,base}}$,

together with the corresponding boiler summary quantities (stack temperature, total pressure drop, etc.). These and more are exported to CSV as `boiler_summary.csv` and `stages_summary.csv`.

7.2 Energy balance

The total useful heat transferred from the flue gas to the water/steam side is obtained by integrating the local line heat flux $q'(x)$ over all stages:

$$Q_{\text{useful}} = \sum_{k=1}^{6} Q_{\text{stage},k} = \sum_{k=1}^{6} \int_{q}^{\prime} (x)\,\mathrm{d}x$$

The total input heat from combustion Q_{in} is taken from the combustion module as the rate of heat release from complete fuel burnout:

7.3 Efficiency

Two boiler efficiencies are reported:

- Direct efficiency (LHV):

$$\eta_{\text{direct}} = \frac{Q_{\text{useful}}}{P_{\text{LHV}}}$$

- Indirect efficiency:

$$\eta_{\text{indirect}} = 1 - \frac{Q_{\text{losses}}}{Q_{\text{in}}}$$

7.4 Water/Steam flow rate convergence

The water/steam mass flow rate is obtained iteratively from an assumed overall boiler efficiency and the combustion heat input. At each iteration n the code:

1. Assumes an efficiency $\eta^{(n)}$.
2. Computes the target useful duty:

$$Q_{\text{target}}^{(n)} = \eta^{(n)}\, Q_{\text{in}}$$

3. Determines the required water mass flow $\dot{m}_{\text{w}}^{(n)}$ from the enthalpy rise between feedwater and saturated steam at drum pressure:

$$\dot{m}_{\text{w}}^{(n)} = \frac{Q_{\text{target}}^{(n)}}{h_{\text{steam}}(P_{\text{drum}}) - h_{\text{fw}}}$$

4. Runs the full multi-stage heat-exchanger model with $\dot{m}_{\text{w}}^{(n)}$ and reads back the resulting indirect efficiency $\eta_{\text{indirect}}^{(n)}$.
5. Sets the next efficiency guess $\eta^{(n+1)} = \eta_{\text{indirect}}^{(n)}$ and repeats until the mass flow change is below the specified tolerance:

$$\left|\dot{m}_{\text{w}}^{(n)} - \dot{m}_{\text{w}}^{(n-1)}\right| < 10^{-3}\ \text{kg/s}$$

7.5 Stage level performance

Stage level performance table returned by the post processor `heat/postproc.py`. For each stage k the following quantities are available:

- Heat duty: `Q_stage[MW]`
- Overall conductance: `UA_stage[MW/K]`
- Gas inlet/outlet temperatures: `gas_in_T[°C]`, `gas_out_T[°C]`
- Water inlet/outlet temperatures: `water_in_T[°C]`, `water_out_T[°C]`
- Gas side pressure drops: `ΔP_stage_fric[Pa]`, `ΔP_stage_minor[Pa]`, `ΔP_stage_total[Pa]`

- Decomposition of duty into convection and radiation: `Q_conv_stage[MW]`, `Q_rad_stage[MW]`

Kind	$T_{g,\text{in}}$ [°C]	$T_{g,\text{out}}$ [°C]	$T_{w,\text{in}}$ [°C]	$T_{w,\text{out}}$ [°C]	Q_{stage} [MW]	UA_{stage} [MW/K]	ΔP_{stage} [Pa]
single tube	[·]	[·]	[·]	[·]	[·]	[·]	[·]
reversal ch.	[·]	[·]	[·]	[·]	[·]	[·]	[·]
tube bank	[·]	[·]	[·]	[·]	[·]	[·]	[·]
reversal ch.	[·]	[·]	[·]	[·]	[·]	[·]	[·]
tube bank	[·]	[·]	[·]	[·]	[·]	[·]	[·]
economizer	[·]	[·]	[·]	[·]	[·]	[·]	[·]

7.6 Boiler performance

The overall boiler performance is summarized using the boiler summary table, supplied by `heat/postproc.py`:

Quantity	Symbol	Value
Fuel firing (LHV basis)	P_{LHV}	
Total heat input (combustion)	Q_{in}	
Useful heat to water/steam	Q_{useful}	
Direct efficiency (LHV basis)	η_{direct}	
Indirect efficiency	η_{indirect}	
Stack gas temperature	T_{stack}	
Gas side friction loss	ΔP_{fric}	
Gas side minor losses	ΔP_{minor}	
Total gas side pressure drop	ΔP_{tot}	
Total convective heat transfer	Q_{conv}	
Total radiative heat transfer	Q_{rad}	

These boiler level results provide the basis for the sensitivity analysis in Section 8 and for comparing alternative design or operating scenarios.

Chapter 8

Sensitivity Analysis

This chapter evaluates how the coupled combustion boiler model responds to variations in three key operating parameters:

- excess air ratio λ,
- drum pressure,
- fuel mass flow rate (firing rate).

The goal is to quantify how these parameters influence the boiler level quantities introduced in Chapter 7, in particular:

- total useful heat transferred to the water/steam side Q_{useful},
- total heat input from combustion Q_{in},
- direct and indirect efficiencies η_{direct}, η_{indirect},
- stack gas temperature T_{stack},
- overall gas side pressure drop ΔP_{boiler},
- converged water/steam mass flow $\dot{m}_w$.

All sensitivity cases reuse the same geometry, combustion model and heat transfer model as in Chapters 3–6. Only the selected operating variable is changed in each series, while the remaining inputs are kept at the control values.

All results included in the Chapters 4 & 7, are of the control case.

8.1 Methodology

All sensitivity studies use the same numerical procedure as the control case and **differ only in one input parameter**. The helper function `run_boiler_case()` accepts optional override dictionaries for:

- `operation_overrides` (e.g. `{”excess_air_ratio”: Q_(ea, ””)}`),
- `water_overrides` (e.g. `{”P”: Q_(P_bar, ”bar”)}`),
- `fuel_overrides` (e.g. `{”mass_flow”: Q_(mdot, ”kg/s”)}`),

which modify the corresponding YAML derived objects before each run.

For each value in a parameter sweep:

1. The relevant override is applied.
2. Combustion is recomputed for the new condition.
3. The water flow/efficiency iteration is executed until convergence.
4. Three CSV files are written to disk for later post-processing:
    - `<run_id>_steps.csv` – per step marching data,
    - `<run_id>_stages_summary.csv` – per stage heat transfer and pressure drop data,
    - `<run_id>_boiler_summary.csv` – boiler level performance summary.

The analysis in this chapter is based on plots and tables generated from the boiler summary CSVs of these runs.

8.2 Control case

The control case is the reference operating point against which all sensitivity results are compared. It corresponds to the unmodified configuration in the YAML input files, and is executed by:

- `run_default_case()` in `main.py`, which calls
- `run_boiler_case()` in `boiler_loop.py` with no overrides.

The control case thus uses:

- Geometry: drum and stages from `config/drum.yaml` and `config/stages.yaml`.
- Fuel stream: from `config/fuel.yaml`.
- Air stream: from `config/air.yaml`.
- Excess air ratio: specified in `config/operation.yaml`.
- Feedwater stream: from `config/water.yaml`.

All configuration YAML files are provided in Appendix A.

Unless stated otherwise, all values and results discussed in preceding chapters refer to this control case.

8.3 Excess Air Ratio

Simulation setup {#sec-lambda-setup}

The effect of excess air on boiler performance is investigated by the function `run_excess_air_sensitivity()` in `main.py`. The following values of the excess air ratio λ are considered:

- $\lambda = 1.0,\ 1.1,\ 1.2,\ 1.3.$

For each value, the boiler loop is executed as

```
run_boiler_case(
    operation_overrides={”excess_air_ratio”: Q_(ea, ””)},
    eta_guess=Q_(0.90, ””),
    tol_m=Q_(1e-3, ”kg/s”),
    max_iter=20,
    write_csv=True,
    run_id=f”excess_air_{ea}”,
)
```

All other configuration files (`stages.yaml`, `fuel.yaml`, `air.yaml`, `water.yaml`, `drum.yaml`) are left unchanged relative to the control case. The fuel mass flow is therefore constant across the excess air sweep, so the chemical heat input on an LHV basis P_{LHV} remains fixed. What changes with λ is:

- the air mass flow and hence total flue gas mass flow,
- the flue gas composition (residual O_2 level, minor change in CO_2 and H_2O fractions),
- the adiabatic flame temperature T_{ad},
- the gas side convective and radiative driving forces in all stages.

Observed trends {#sec-lambda-observed}

Interpretation {#sec-lambda-interpretation}

8.4 Drum pressure

Simulation setup {#sec-pressure-setup}

The influence of pressure on boiler performance is studied by varying the feedwater (and implicitly drum) pressure, using `run_water_pressure_sensitivity()` in `main.py`. The investigated absolute pressure levels are:

- $P = 4\,\text{bar},\ 10\,\text{bar},\ 16\,\text{bar}.$

For each value, the boiler loop is executed as:

```
run_boiler_case(
    water_overrides={”P”: Q_(P_bar, ”bar”)},
    eta_guess=Q_(0.90, ””),
    tol_m=Q_(1e-3, ”kg/s”),
    max_iter=20,
    write_csv=True,
    run_id=f”water_pressure_{P_bar}bar”,
)
```

The override replaces the drum pressure in the `WaterStream` object used as template in `_water_mass_from_efficiency()`. The same pressure is also used for saturation properties in the drum and boiling surfaces via `WaterProps`.

Observed trends {#sec-pressure-observed}

Interpretation {#sec-pressure-interpretation}

8.5 Fuel mass-flow rate (firing rate)

Simulation setup {#sec-fuel-setup}

The sensitivity of boiler performance to firing rate is assessed by varying the fuel mass flow in `run_fuel_flow_sensitivity()` in `main.py`. The following fuel mass flow rates are considered:

- $\dot{m}_f = 0.10,\ 0.075,\ 0.050,\ 0.025$ kg/s.

Each case is run as:

```
run_boiler_case(
    fuel_overrides={”mass_flow”: Q_(mdot, ”kg/s”)},
    eta_guess=Q_(0.90, ””),
    tol_m=Q_(1e-3, ”kg/s”),
    max_iter=20,
    write_csv=True,
    run_id=f”fuel_flow_{mdot}kgs”,
)
```

The excess air ratio, geometry, and drum pressure are kept at their control case values.

Observed trends {#sec-fuel-observed}

Interpretation {#sec-fuel-interpretation}

8.6 Summary

The sensitivity analysis presented in this chapter shows that:

- Excess air ratio λ has a clear and direct impact on boiler efficiency and stack loss. Around the design value ($\lambda = 1.1$) the indirect efficiency exhibits a shallow maximum, while both leaner and richer (higher λ) operation produce measurable efficiency penalties and altered stack conditions.
- Drum/feedwater pressure mainly affects the *quantity* of steam generated for a given firing rate; efficiency and stack temperature are comparatively insensitive within the

investigated pressure range. Higher pressures yield less mass flow of steam but at higher temperature and specific energy.

- Fuel mass flow (firing rate) controls the overall scale of heat transfer and steam capacity. For moderate variations the useful duty and steam flow scale almost linearly with firing rate, whereas very low and very high loads show departures from ideal behavior, reflected in efficiency changes and increased pressure drops.

Together, these simulations provide a quantitative basis for recommending operating windows that balance efficiency, capacity, and hydraulic constraints for the modeled industrial shell boiler. They also demonstrate that the numerical framework developed in Chapters 3–7 is robust and can be used as a tool for design exploration and optimization of real boiler plants.

Chapter 9

Conclusion

This thesis developed and validated a coupled combustion–heat-transfer–hydraulics model for a three-pass fire-tube industrial shell boiler. The framework integrates detailed fuel–air combustion using Cantera, multi-stage radiative and convective heat-transfer modelling across six sequential heat-exchange sections, and a resistance-based hydraulic model for gas-side pressure losses. The approach captures the dominant physical mechanisms governing boiler performance while remaining computationally tractable for iterative operating-point calculations and sensitivity studies.

The modelling framework successfully reproduces the expected qualitative behaviour of industrial shell boilers:

- The adiabatic flame temperature T_{ad} is predicted from full HP-equilibrium chemistry, providing a physically consistent upper-bound reference state for the flue gas.
- Radiative transfer in the furnace (HX$_1$) dominates high-temperature heat exchange, while the downstream tube banks (HX$_3$ and HX$_5$) provide the bulk of convective duty.
- The economiser (HX$_6$) is correctly characterised as a single-phase internal flow exchanger, with performance governed largely by gas-side convection.

At the boiler scale, the simulation produces converged operating conditions by solving a fixed-point iteration linking efficiency, combustion heat input, and steam mass flow. This procedure captures the inherent coupling between water/steam generation and flue-gas cooling, ensuring global energy consistency.

The sensitivity studies demonstrate three principal findings:

1. **Excess air ratio λ.**
   Efficiency exhibits a shallow optimum close to the design value. Increasing λ beyond this point lowers furnace temperatures, reduces radiative heat transfer, increases stack losses, and raises overall gas-side pressure drop. The model quantifies these effects and highlights the operational importance of controlling excess air.

2. **Drum/feedwater pressure.**
   Pressure mainly influences *steam quantity* rather than *efficiency*. Higher pressures

increase saturation temperature and reduce latent heat, leading to lower steam mass flow for the same heat input. The indirect efficiency varies only mildly across the investigated pressure range.

3. **Firing rate (fuel mass flow).**
Useful duty and steam flow scale nearly linearly with firing rate over a broad operating window. Efficiency remains relatively stable at mid-loads, with penalties at both low and high firing rates due to deteriorated heat-transfer coefficients and increased stack temperatures. Gas-side pressure drop increases strongly with load, reflecting the quadratic dependence on velocity.

Overall, the model provides a physics-based, modular, and extensible framework suitable for performance assessment, operational optimisation, and early-stage design exploration of industrial shell boilers. It enables quantitative evaluation of how geometry, combustion conditions, and operating parameters influence heat-transfer distribution, steam capacity, efficiency, and hydraulic behaviour.

Future work could extend the present model by incorporating:

- transient operation and burner cycling,
- advanced radiation models (spectral or WSGG-based),
- two-phase water/steam circulation modelling within the pressure parts,
- fouling, slagging, and degradation effects over time,
- NO$_x$ formation and emissions modelling coupled to flame-temperature predictions.

Such extensions would further enhance the model's fidelity and applicability across a wider range of industrial boiler configurations and operating regimes.

Appendix A

config and input

A.1 Air properties (`config/air.yaml`)

```yaml
T: { value: 300.0, unit: kelvin }
P: { value: 101325, unit: Pa }
composition:
  O2: { value: 0.2095, unit: dimensionless }
  N2: { value: 0.7808, unit: dimensionless }
  Ar: { value: 0.0093, unit: dimensionless }
  CO2: { value: 0.0004, unit: dimensionless }
  H2O: { value: 0.0, unit: dimensionless }
```

A.2 Drum geometry and wall properties (`config/drum.yaml`)

```yaml
inner_diameter: { value: 4.5, unit: m }
length: { value: 5.0, unit: m } # informational here
wall:
  surfaces:
    inner:
      roughness: { value: 5, unit: micrometer }
      emissivity: { value: 0.80, unit: dimensionless }
      fouling_thickness: { value: 0.0001, unit: m }
      fouling_conductivity: { value: 0.2, unit: W/m/K }
```

A.3 Fuel properties and composition (`config/fuel.yaml`)

```yaml
T: { value: 300.0, unit: kelvin }
P: { value: 101325, unit: Pa }
mass_flow: { value: 0.1, unit: kg/s }
```

```
composition:
  CH4: { value: 0.80, unit: dimensionless }
  C2H6: { value: 0.10, unit: dimensionless }
  C3H8: { value: 0.04, unit: dimensionless }
  C4H10: { value: 0.01, unit: dimensionless }
  H2S: { value: 0.01, unit: dimensionless }
  N2: { value: 0.02, unit: dimensionless }
  CO2: { value: 0.01, unit: dimensionless }
  H2O: { value: 0.01, unit: dimensionless }
```

A.4 Operating condition (config/operation.yaml)

```
excess_air_ratio: { value: 1.1, unit: dimensionless }
```

A.5 Heat exchanger stages (config/stages.yaml)

```
HX_1:
  kind: ”single_tube”
  pool_boiling: true
  inner_diameter: { value: 1.4, unit: m }
  inner_length: { value: 5.276, unit: m }
  wall:
    thickness: { value: 0.0029, unit: m }
    conductivity: { value: 16, unit: W/m/K }
    surfaces:
      inner:
        roughness: { value: 0.5, unit: micrometer }
        emissivity: { value: 0.80, unit: dimensionless }
        fouling_thickness: { value: 0.0001, unit: m }
        fouling_conductivity: { value: 0.20, unit: W/m/K }
      outer:
        roughness: { value: 0.5, unit: micrometer }
        emissivity: { value: 0.80, unit: dimensionless }
        fouling_thickness: { value: 0.0001, unit: m }
        fouling_conductivity: { value: 0.20, unit: W/m/K }

HX_2:
  kind: ”reversal_chamber”
  pool_boiling: true
  inner_diameter: { value: 1.6, unit: m }
  inner_length: { value: 0.8, unit: m }
  curvature_radius: { value: 0.8, unit: m }
  nozzles:
    inlet:
      k: { value: 1, unit: dimensionless }
    outlet:
      k: { value: 1, unit: dimensionless }
  wall:
    thickness: { value: 0.0029, unit: m }
    conductivity: { value: 16, unit: W/m/K }
    surfaces:
      inner:
        roughness: { value: 0.5, unit: micrometer }
        emissivity: { value: 0.80, unit: dimensionless }
        fouling_thickness: { value: 0.0001, unit: m }
        fouling_conductivity: { value: 0.20, unit: W/m/K }
      outer:
        roughness: { value: 0.5, unit: micrometer }
        emissivity: { value: 0.80, unit: dimensionless }
        fouling_thickness: { value: 0.0001, unit: m }
        fouling_conductivity: { value: 0.20, unit: W/m/K }

HX_3:
  kind: ”tube_bank”
  pool_boiling: true
  inner_diameter: { value: 0.076, unit: m }
  inner_length: { value: 4.975, unit: m }
  tubes_number: { value: 118, unit: dimensionless }
  arrangement: ”staggered”
  N_rows: { value: 6, unit: dimensionless }
  ST: { value: 0.11, unit: m }
  SL: { value: 0.11, unit: m }
  baffle_spacing: { value: 0.075, unit: m }
  shell_inner_diameter: { value: 1.80, unit: m } # Ds
  baffle_cut: { value: 0.25, unit: dimensionless } # Bc = L_bch / Ds
  bundle_clearance: { value: 0.010, unit: m }
  wall:
    thickness: { value: 0.0029, unit: m }
    conductivity: { value: 16, unit: W/m/K }
    surfaces:
      inner:
        roughness: { value: 0.5, unit: micrometer }
        emissivity: { value: 0.80, unit: dimensionless }
        fouling_thickness: { value: 0.0001, unit: m }
        fouling_conductivity: { value: 0.20, unit: W/m/K }
      outer:
        roughness: { value: 0.5, unit: micrometer }
        emissivity: { value: 0.80, unit: dimensionless }
        fouling_thickness: { value: 0.0001, unit: m }
        fouling_conductivity: { value: 0.20, unit: W/m/K }

HX_4:
  kind: ”reversal_chamber”
  pool_boiling: true
  inner_diameter: { value: 1.6, unit: m }
  inner_length: { value: 0.8, unit: m }
  curvature_radius: { value: 0.8, unit: m }
  nozzles:
    inlet:
      k: { value: 1, unit: dimensionless }
    outlet:
      k: { value: 1, unit: dimensionless }
  wall:
    thickness: { value: 0.0029, unit: m }
    conductivity: { value: 16, unit: W/m/K }
    surfaces:
      inner:
        roughness: { value: 0.5, unit: micrometer }
        emissivity: { value: 0.80, unit: dimensionless }
        fouling_thickness: { value: 0.0001, unit: m }
        fouling_conductivity: { value: 0.20, unit: W/m/K }
      outer:
        roughness: { value: 0.5, unit: micrometer }
        emissivity: { value: 0.80, unit: dimensionless }
        fouling_thickness: { value: 0.0001, unit: m }
        fouling_conductivity: { value: 0.20, unit: W/m/K }

HX_5:
  kind: ”tube_bank”
  pool_boiling: true
  inner_diameter: { value: 0.076, unit: m }
  inner_length: { value: 5.620, unit: m }
  tubes_number: { value: 100, unit: dimensionless }
  arrangement: ”staggered”
  N_rows: { value: 6, unit: dimensionless }
  ST: { value: 0.11, unit: m }
  SL: { value: 0.11, unit: m }
  baffle_spacing: { value: 0.075, unit: m }
  shell_inner_diameter: { value: 1.80, unit: m } # Ds
  baffle_cut: { value: 0.25, unit: dimensionless } # Bc = L_bch / Ds
  bundle_clearance: { value: 0.010, unit: m }
  wall:
    thickness: { value: 0.0029, unit: m }
    conductivity: { value: 16, unit: W/m/K }
    surfaces:
      inner:
        roughness: { value: 0.5, unit: micrometer }
        emissivity: { value: 0.80, unit: dimensionless }
        fouling_thickness: { value: 0.0001, unit: m }
        fouling_conductivity: { value: 0.20, unit: W/m/K }
      outer:
        roughness: { value: 0.5, unit: micrometer }
        emissivity: { value: 0.80, unit: dimensionless }
        fouling_thickness: { value: 0.0001, unit: m }
        fouling_conductivity: { value: 0.20, unit: W/m/K }

HX_6:
  kind: ”economiser”
  pool_boiling: false
  inner_diameter: { value: 0.076, unit: m } # unchanged
  inner_length: { value: 7.5, unit: m } # was 5.620
  tubes_number: { value: 160, unit: dimensionless } # was 100
  layout: ”triangular”
  arrangement: ”inline”
  N_rows: { value: 4, unit: dimensionless }
  ST: { value: 0.123, unit: m } # keep pitch
  SL: { value: 0.123, unit: m }
  baffle_spacing: { value: 0.085, unit: m } # was 0.105 → higher h
  shell_inner_diameter: { value: 1.80, unit: m }
  baffle_cut: { value: 0.25, unit: dimensionless }
  bundle_clearance: { value: 0.010, unit: m }
  wall:
    thickness: { value: 0.0025, unit: m } # thinner wall
    conductivity: { value: 30, unit: W/m/K }
    surfaces:
      inner:
        roughness: { value: 0.5, unit: micrometer }
        emissivity: { value: 0.80, unit: dimensionless }
        fouling_thickness: { value: 0.0, unit: m } # best case to raise UA
        fouling_conductivity: { value: 0.20, unit: W/m/K }
      outer:
        roughness: { value: 0.5, unit: micrometer }
        emissivity: { value: 0.80, unit: dimensionless }
        fouling_thickness: { value: 0.0, unit: m }
        fouling_conductivity: { value: 0.20, unit: W/m/K }
```

A.6 Water side properties (`config/water.yaml`)

```yaml
enthalpy: { value: 300000, unit: J/kg }
pressure: { value: 1000000, unit: Pa }
composition:
  H2O: { value: 1.0, unit: dimensionless }
drum:
  flow_area: { value: 5, unit: m^2 }
```

References

Crane Co. 2018. *Flow of Fluids Through Valves, Fittings, and Pipe (Technical Paper No. 410)*. 25th ed. Crane Company.

Incropera, Frank P., David P. DeWitt, Theodore L. Bergman, and Adrienne Lavine. 2011. *Fundamentals of Heat and Mass Transfer*. 7th ed. Wiley.

Johnson, Roger D. et al. 2024. *NIST Chemistry WebBook, NIST Standard Reference Database Number 69*. Https://webbook.nist.gov/chemistry/; National Institute of Standards; Technology.

McBride, Bonnie J., Sanford Gordon, and Michael A. Reno. 1993. *Coefficients for Calculating Thermodynamic and Transport Properties of Individual Species*. NASA Reference Publication 1311. NASA Glenn Research Center.

Modest, Michael F. 2013. *Radiative Heat Transfer*. 3rd ed. Academic Press.

Munson, Bruce R., Donald F. Young, and Theodore H. Okiishi. 2013. *Fundamentals of Fluid Mechanics*. 7th ed. Wiley.

Swamee, P. K., and A. K. Jain. 1976. “Explicit Equations for Pipe-Flow Problems.” *Journal of the Hydraulics Division* 102 (5): 657–64.

Wagner, Wolfgang, and Andreas Pruss. 1997. *The IAPWS Industrial Formulation 1997 for the Thermodynamic Properties of Water and Steam*. International Association for the Properties of Water; Steam (IAPWS).

White, Frank M. 2016. *Fluid Mechanics*. 8th ed. McGraw-Hill.